INCREASED ROUGHNESS IN REINFORCED CONCRETE BOX CULVERTS

By

ADAM SAMUEL HILL

A thesis submitted in partial fulfillment of
the requirements for the degree of

MASTER OF SCIENCE IN CIVIL ENGINEERING

WASHINGTON STATE UNIVERSITY
Department of Civil and Environmental Engineering

AUGUST 2006

To the Faculty of Washington State University:

The members of the Committee appointed to examine the thesis of ADAM SAMUEL HILL find it satisfactory and recommend that it be accepted.

Chair

ACKNOWLEDGMENT

I would like to thank my committee chair, Dr. Rollin Hotchkiss, for his support, guidance, and teaching throughout the development of this thesis. I would also like to thank committee members Dr. Michael Barber and Dr. Marc Beutel for their valuable comments and review. Dr. David Admiraal at the University of Nebraska—Lincoln gave advice on the development of the construction of the model design and led to the avoidance of headaches during experimental testing. Undergraduate assistants Kayla Culmer and Mike Miraglio provided assistance in the construction and testing of the experimental models. With their help, I was able to complete the research in a timely matter. The support from my peers in Albrook Hyrdaulics Laboratory kept me motivated and in high spirits throughout the whole research process. My family has continued to give me unwavering support and they gave me my basis for the drive and motivation behind this research. I would especially like to thank my wife, Brittany Stuckel-Hill, for her unending love, support, and patience throughout this whole process. If it wasn't for her, I would not be writing this thesis right now.

The ideas of Kevin Donahoo, Hydraulic Engineer, Roadway Design Division, Nebraska Department of Roads, were the basis of the designs researched. The project was fully funded by the Nebraska Department of Roads.

INCREASED ROUGHNESS IN REINFORCED CONCRETE BOX CULVERTS

Abstract

by Adam Samuel Hill, M.S.
Washington State University
August 2006

Chair: Rollin H. Hotchkiss

The purpose of this experimental investigation was to determine the extent to which trapezoidal-shaped corrugations placed within a barrel of a reinforced concrete box culvert decreased water velocity within the barrel.

Flow measurements were conducted in a tilting flume in Albrook Hydraulics Laboratory at Washington State University in Pullman, WA, using a half-scale simulation of the corrugations expected to be used in the field. Discharges ranged from 24.1-144 L/s and slopes ranged from 0.3-10.1 percent. Tests were also conducted in a flume in Sloan Teaching Laboratory using a quarter-scale simulation, where discharges ranged from 13.9-97.1 L/s. The flume slope was zero. Depths were measured using a point gage at seven different locations in both flumes.

Sixty-eight tests were used to determine the Manning 'n' value. Manning's 'n' is inversely proportional to the submergence ratio and to the aspect ratio. Experimental errors in the determination of Manning's 'n' ranged from 4.3-10 percent. Manning's 'n' values for replication tests were within 3.2 percent of the original test.

Undular jumps did not occur in experimental testing; however, hydraulic jumps did form in some experiments upon initially reaching the corrugations. The jumps are caused by the change in critical slope due to the increase in roughness. Three different flow situations were observed during upstream supercritical flow experiments.

Velocities within the corrugations decreased 44-66 percent compared to upstream supercritical velocity. Broken-back Culvert Analysis Program (BCAP) outputs compared reasonably well with experimental results within the corrugations if inputs were set so the hydraulics at the break were the same as the upstream experimental data. The program suggests a hydraulic jump will form within the corrugated outlet section of a broken-back culvert.

Velocity data were collected using an Acoustic Doppler Velocimeter (ADV) and compared with a study by Ead et al. (2000). The velocity profile was found to fit a log law profile using the Prandtl equation for rough turbulent flow for data points above the corrugation crest. The shear velocity was 2.9 times higher and the Nikuradse equivalent sand roughness was 100 times higher than values found by Ead et al. (2000).

TABLE OF CONTENTS

Page

LIST OF FIGURES

Page

LIST OF TABLES

Page

NOTATION

The following notations are used in this thesis:

n	=	Manning's roughness coefficient
y_c	=	Critical depth [L]
z	=	Corrugation height [L]
φ, S	=	Slope
V	=	Velocity [LT^{-1}]
R	=	Hydraulic radius (A/P) [L]
Q	=	Discharge [L^3T^{-1}]
A	=	Cross-sectional area of flume/culvert [L^2]
y	=	Water depth [L]
b	=	Flume/culvert width [L]
R_s	=	Submergence ratio (y/z)
R_A	=	Aspect ratio (b/y)
Fr	=	Froude number $(V/(gy)^{1/2})$
g	=	Gravitational constant [LT^{-2}]
Fr_B	=	"Barrier" Froude number
Q^*	=	Dimensionless discharge $(10^{-9}Qg^{1/3}\nu^{-5/3})$
ν	=	Kinematic viscosity [L^2T^{-1}]
u	=	Streamwise velocity [LT^{-1}]
y_0	=	Vertical depth position [L]
u_*	=	Shear velocity [LT^{-1}]
k_s	=	Nikuradse equivalent sand roughness [L]

κ = von Karman constant

Δu = velocity change over reference shift [LT^{-1}]

CHAPTER ONE

INTRODUCTION AND BACKGROUND

Culverts are important hydraulic structures used to pass water under roadways. In certain situations, a culvert may be required to have a steep slope, which increases flow velocity. High velocity at a culvert outlet may scour the channel bed, causing erosion of the natural channel.

For years, the Nebraska Department of Roads (NDOR) has been using the Broken-back Culvert Analysis Program, also known as BCAP (Shafer and Hotchkiss 1998). The program predicts that in larger broken-back reinforced concrete box (RCB) culverts, which would otherwise be designed with an expensive external energy dissipater, the culvert exit velocity can be effectively reduced by increasing the Manning's roughness coefficient to approximately 0.035 within the outlet section of the culvert.

It is theorized that placing trapezoidal-shaped corrugations similar to the shape of bridge decking inside a RCB culvert will increase Manning's 'n' to the desired roughness. The increased roughness is expected to significantly reduce velocities within the culvert, sometimes triggering a hydraulic jump.

The objectives of this research are to:

1) Experimentally determine the Manning's 'n' of the proposed corrugations within a RCB culvert.
2) Attempt to create an undular jump within the experimental flume as expected by BCAP predictions.

3) Determine the impact the increased roughness has on flow conditions, including flow in a broken-back culvert if the corrugations are applied to the outlet section, as well as if BCAP can be used to model the corrugations in a broken-back culvert.
4) Determine if the corrugations follow a log law velocity profile and compare experimental data with a previously published study on corrugated metal pipe (CMP) culverts.

CHAPTER TWO

PREVIOUS WORK

Previous research related to this subject has focused on skimming flow in stepped spillways and corrugated pipes for use as culverts. Recent research has looked at dissipating energy in culverts by forcing a hydraulic jump within the barrel using end weirs (Hotchkiss et al. 2005). This chapter will briefly review skimming flow and corrugated culverts (see Appendix A for extended literature review on skimming flow).

Skimming Flow

Two main types of flow exist in stepped spillways. Nappe flow generally occurs on larger steps with small discharges and on relatively mild-sloped spillways (Pegram et al. 1999). Nappe flow is described as having an air pocket at each step (Ohtsu et al. 2004). In contrast, skimming flow generally occurs on steep-sloped spillways with small steps relative to the water depth (Pegram et al. 1999). Skimming flow is described as having a so-called "pseudo-bottom" along the step edges with circulating eddies formed at each step (Ohtsu et al. 2004).

Several findings have been developed from previous work. Boes and Hager (2003) determine the transition between skimming flow and nappe flow to be dependent on critical depth y_c, step height z, and spillway slope φ in the following equation:

$$\frac{y_c}{z} = 0.91 - 0.14 \tan \phi \qquad (1)$$

Ohtsu et al. (2004) find the friction factor in a stepped channel to be anywhere from 5.5 to 13 times that of a smooth channel with similar slope and material.

Corrugated Culverts

Corrugated pipe has been used for drainage structures for several decades. Steel pipe is typically used due to the large strength to dead weight ratio, which allows for lightweight pipe. Lightweight pipe is easy to install, which results in a low cost per unit length of pipe (Smith 1988). Other advantages include a large availability of sizes and shapes and fast assembly in the field (Ring 1984). This increase in availability was widespread in the 1960s and 1970s, when corrugated pipe was found to be an alternative to short-span bridges (Moore et al. 1995). Major disadvantages include decreased flow due to the corrugations, loss of metal through abrasion, pipe corrosion, and a controlled backfill in order to have proper support from the soil (Ring 1984).

Sinusoidal corrugations have gathered the most attention from researchers due to its high availability and widespread use. Smith (1988) determined the Manning's 'n' for standard corrugated pipe flowing full at high Reynolds numbers to range from 0.013-0.025. Ead et al. (2000) studied the velocity field in turbulent open-channel flow in a corrugated pipe and found the Manning's 'n' to equal 0.023. Velocity profiles were found to follow the log law and can be described by the Prandtl equation for rough turbulent flow. The Nikuradse equivalent sand roughness was found to equal the amplitude of the corrugations.

CHAPTER THREE

EXPERIMENTAL SETUP

Tilting Flume

Flow measurements were conducted in Albrook Hydraulics Laboratory at Washington State University in Pullman, WA (see Figure 1). Wood cut to the shape of bridge decking ("Bridge" 2006) was used as a half-scale simulation of the concrete forms expected to be used in the field (see Figure 2). Spacing between corrugations was set using a half-scale distance as well.

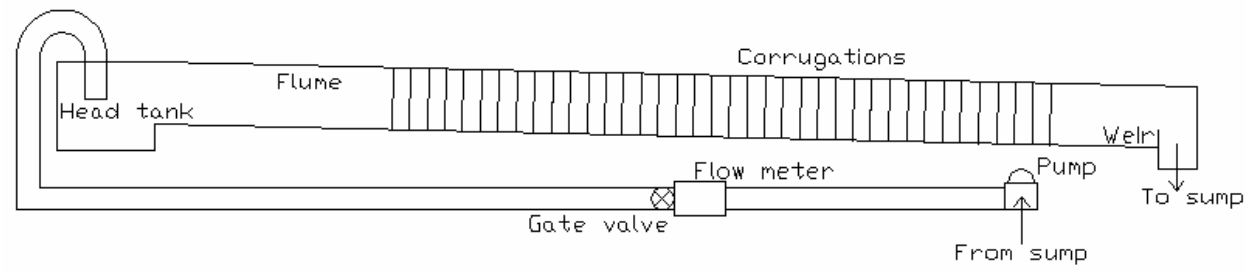

(a)

(b)

Figure 1. (a) Schematic of elevation view (not to scale) and (b) photograph looking upstream of tilting flume setup in Albrook Hydraulics Laboratory.

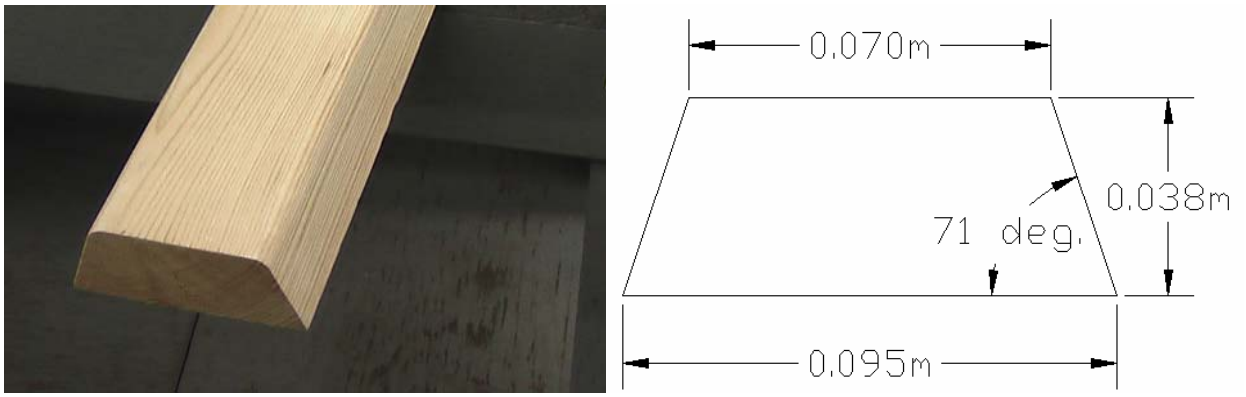

Figure 2. (a) Photograph and (b) dimensions of half-scale wood corrugations. Flow is from left to right over the corrugations in this elevation view.

The trapezoidal wood corrugations were primed and painted to protect against warping and water retention and nailed to a concrete board base. Concrete board was placed in the bottom of the rectangular tilting flume 21.06 meters long, 0.90 meters wide, and 0.53 meters deep. Wood corrugations on both flume walls were attached to the bottom corrugations by angle braces, and all wall corrugations were attached to the flume with C-clamps. This bracing protected against buoyancy effects and maintained perpendicularity between the planes of the side and bottom corrugation faces. Corrugations began 5.00 meters downstream of water entering the flume to allow flow to fully develop before encountering the corrugations. Seventy-two corrugations were placed in the flume with a total distance of 13.62 meters. The side corrugations caused the flume width to become 0.82 meters at the corrugation crests. A variable-height weir was located 2.44 meters beyond the final corrugation at the end of the flume. The weir was set to remove drawdown or backwater effects and thus facilitate measurements.

Depth measurements were collected at points upstream of, within, and downstream of corrugations (see Table 1 and Figure 3). Depths were measured at both the crest and the trough within corrugations. Uniform flow prevailed over the corrugation reach as a whole. Depths

were measured at the centerline of the flume using a point gage connected to a gantry system above the flume.

Table 1. Depth measurement locations in tilting flume.

Measurement #	Location (from head tank)	Description
1	3.05 m	Upstream from corrugations
2	4.88 m	Upstream from corrugations
3	6.09 m	Corrugation trough
3c	6.19 m	Corrugation crest
4	12.57 m	Corrugation trough
4c	12.67 m	Corrugation crest
5	18.48 m	Corrugation trough
5c	18.57 m	Corrugation crest
6	19.93 m	Downstream from corrugations
7	21.06 m	Weir

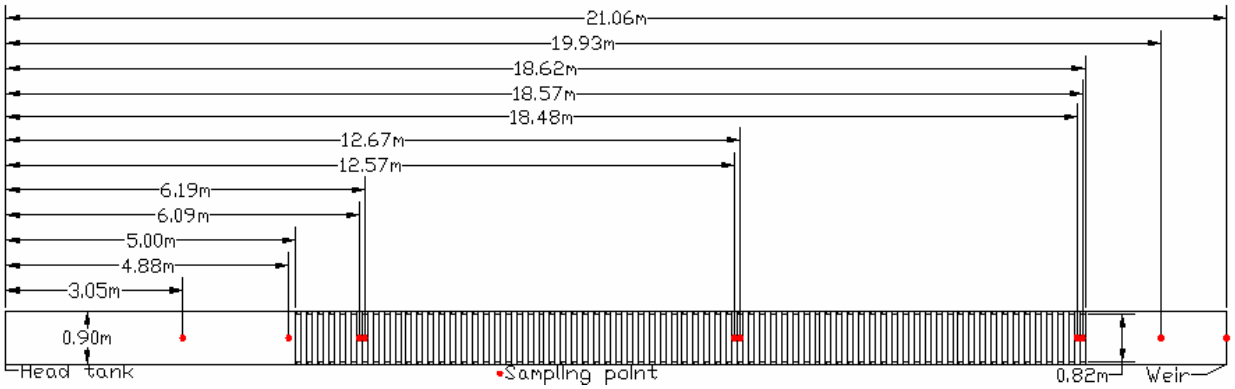

Figure 3. Dimensions and sampling locations of tilting flume. Flow is from left to right in this elevation view.

Water was pumped from the sump to the head tank of the flume and returned to the sump after traveling over the variable-height weir. A combination of a Venturi meter and magnetic flow meter was used to measure discharge. The tilting flume slope was determined using a surveying rod and level. Table 2 shows the slope and discharge used in each experiment.

Table 2. Summary of experimental slopes and discharges in tilting flume.

Experiment #	Slope	Discharge (L/s)	Experiment #	Slope	Discharge (L/s)
1	0.0028	26.9	26	0.04	24.1
2	0.0028	41.3	27	0.04	41.7
3	0.0028	57.7	28	0.04	57.1
4	0.006	28.2	29	0.0463	24.8
5	0.006	42.1	30	0.0463	39.9
6	0.006	42.1	31	0.0463	57.1
7	0.006	57.7	32	0.1008	140.
8	0.009	26.9	33	0.1008	111
9	0.009	41.7	34	0.1008	81.6
10	0.009	57.4	35	0.1008	53.2
11	0.0118	27.6	36	0.08	56.6
12	0.0118	42.1	37	0.08	83.5
13	0.0118	57.7	38	0.08	111
14	0.015	26.9	39	0.08	137
15	0.015	41.7	40	0.06	143
16	0.015	58.0	41	0.06	113
17	0.0183	28.2	42	0.06	85.2
18	0.0183	42.1	43	0.06	54.4
19	0.0183	57.7	44	0.0388	51.5
20	0.021	28.2	45	0.0388	82.7
21	0.021	42.6	46	0.0388	112
22	0.021	58.0	47	0.0388	140.
23	0.03	25.5	48	0.0235	144
24	0.03	41.3	49	0.0235	114
25	0.03	57.7	50	0.0235	82.4

Sloan Flume

Additional tests were completed in the Sloan Teaching Laboratory at Washington State University in Pullman, WA (see Figure 4). These tests were completed using wood corrugations at quarter-scale. These tests were completed to assure scaling remained consistent between half-scale and quarter-scale models and the full-scale prototype.

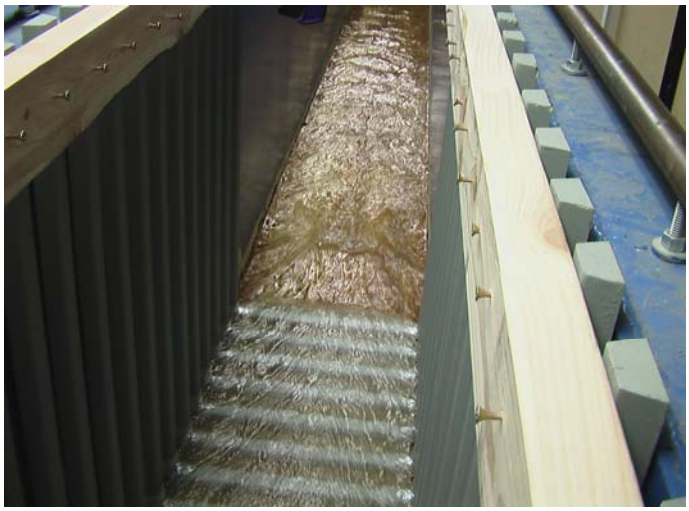

Figure 4. Photograph looking downstream of Sloan flume experimental setup.

Similar strategies were used to prepare the flume for testing. The flume used had dimensions of 14.08 meters long by 0.45 meters wide by 0.90 meters high. Corrugations began 3.07 meters downstream of water entering the flume to allow flow to fully develop before encountering the corrugations. Water entered the flume beneath a sluice gate. Sixty-two corrugations were placed in the flume through a total distance of 5.86 meters. The side corrugations caused the flume width to become 0.41 meters at the corrugation crests. The flume terminated in a free drop 5.15 meters beyond the final corrugation.

Depth measurements were collected using a point gage system similar to the tilting flume. Depths were measured at the upstream sluice gate and downstream drop, one point each upstream and downstream of the corrugations, and three points within the corrugations (see Table 3 and Figure 5). Depths were measured at both the crest and the trough within corrugations. Depths were measured at the centerline of the flume.

Table 3. Depth measurement locations in Sloan flume.

Measurement #	Location (from head tank)	Description
1	0.00 m	Upstream sluice gate
2	2.08 m	Upstream from corrugations
3	3.62 m	Corrugation trough
3c	3.67 m	Corrugation crest
4	5.71 m	Corrugation trough
4c	5.76 m	Corrugation crest
5	8.67 m	Corrugation trough
5c	8.71 m	Corrugation crest
6	11.71 m	Downstream from corrugations
7	14.08 m	Downstream drop

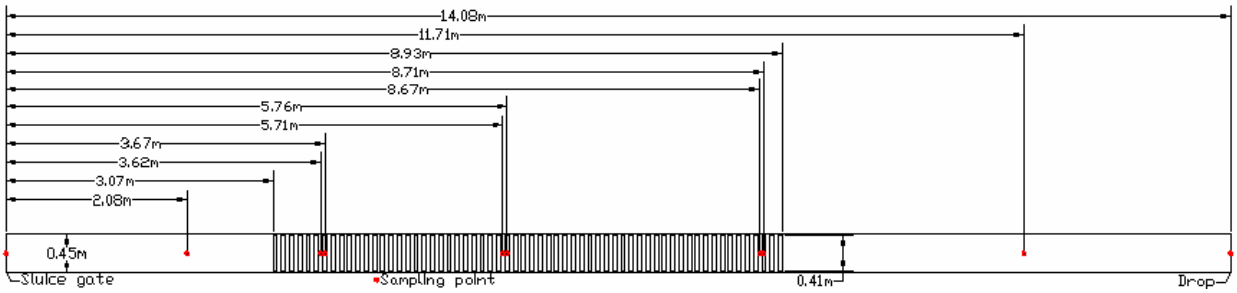

Figure 5. Dimensions and sampling locations of Sloan flume. Flow is left to right in this elevation view.

Water was pumped from the sump to the head tank of the flume and returned to the sump after traveling beyond the downstream drop. A combination of a weigh tank and a stopwatch was used to measure discharge. Discharges ranged from 13.9-97.1 L/s in this zero-percent-sloped flume.

CHAPTER FOUR

DETERMINATION OF MANNING 'N' VALUE

A total of fifty tests in the tilting flume and eighteen tests in the Sloan flume were completed to determine the Manning 'n' value of the corrugations (see Appendix B for raw data). Several flow characteristics were calculated for each depth location, including cross-sectional area, Froude number, and flow velocity, for example (see Appendix C for example). Relationships were established between Manning's 'n' and other flow characteristics. These relationships were scaled to prototype size. Scaling was governed by the Froude number. The prototype Manning's 'n' was found to be a function of the length scale to the $1/6^{th}$ power. All results are independent of the Reynolds number due to flow being in the completely rough regime (see Appendix D for a discussion on scaling Manning's 'n').

Depths from the six measuring locations (three points on the crests of corrugations and three points on the troughs of corrugations) were averaged assuming a bottom channel depth halfway between the crest and trough. These three average depths were used to determine Manning's 'n' using the well known Manning equation in metric units (Jain 2001):

$$V = \frac{1}{n} R^{\frac{2}{3}} \sqrt{S} \qquad (2)$$

Given continuity, Q = VA, (2) can be written as:

$$Q = \frac{1}{n} A R^{\frac{2}{3}} \sqrt{S} \qquad (3)$$

Expanding the area and hydraulic radius terms and solving for *n*, (3) can be written as:

$$n = \frac{(by)^{\frac{5}{3}} (b + 2y)^{\frac{-2}{3}} \sqrt{S}}{Q} \qquad (4)$$

Equation (4) will yield a Manning 'n' value for each measurement. These three values were averaged to find the average Manning's 'n' for the corrugations for each experimental run.

From the results of the experimental runs, both tilting flume tests and Sloan flume tests showed the same relationship. Manning's 'n' was found to be dependent on the submergence ratio and the aspect ratio. Submergence ratio is defined as $R_s = y / z$, where z is the corrugation height, and aspect ratio is defined as $R_A = b / y$. Experiments were split into those with Manning's 'n' greater than 0.030 and those with a Manning's 'n' less than 0.030. Experiments with Manning's 'n' less than 0.030 were assigned a constant Manning's 'n' of 0.024. For experiments with Manning's 'n' greater than 0.030, the following relationship exists (see Figure 6):

$$n = 0.024\left(\frac{R_s}{R_A}\right)^{-0.306} \tag{5}$$

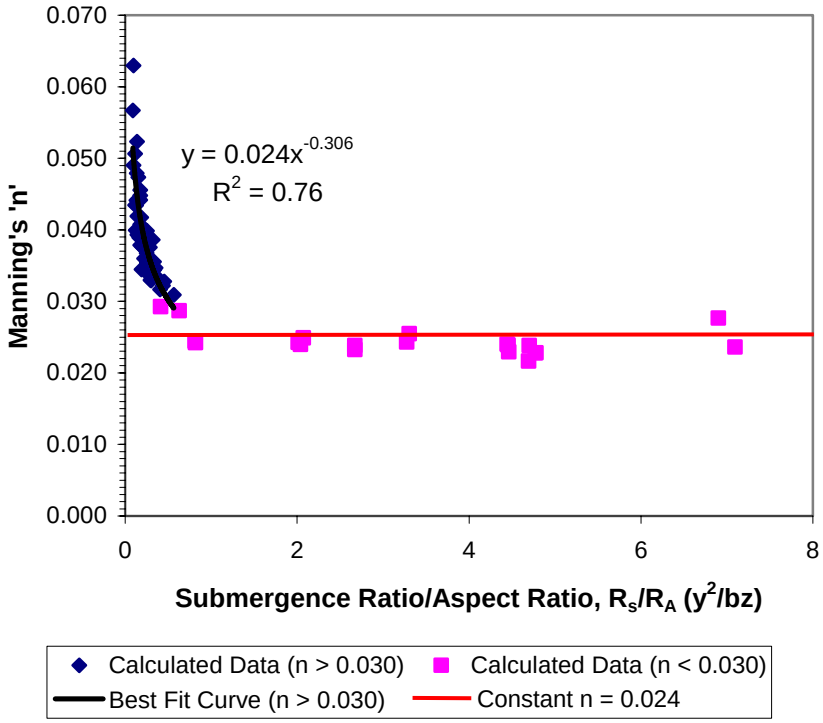

Figure 6. Relationship comparing submergence ratio (R_s) and aspect ratio (R_A) to Manning's 'n'.

This relationship (5), combined with the Manning equation (3), could be used to determine the expected Manning 'n' value for a given discharge and slope in a concrete box culvert (see Appendix E for example).

Errors in the experimentally determined Manning 'n' values ranged from 4.3-10% (see Appendix F for details). Errors were based on the precision of the measurement devices. Replications were completed on four experimental runs. Results were within 3.2% of the initially derived values (see Table 4).

Table 4. Replication experiment results.

Exp.	Slope	Original Discharge (L/s)	Replicate Discharge (L/s)	% Difference	Original 'n'	Replicate 'n'	% Difference
9	0.009	41.6	41.3	*-0.7%*	0.0315	0.0305	*-3.2%*
14	0.015	26.9	27.5	*2.2%*	0.0356	0.0353	*-0.8%*
16	0.015	58.1	57.8	*-0.5%*	0.0315	0.0309	*-1.9%*
22	0.021	58.1	57.8	*-0.5%*	0.0335	0.0335	*0.0%*

CHAPTER FIVE

ATTEMPTS TO CREATE AN UNDULAR JUMP

Undular jumps occur during the transition from supercritical to subcritical flow and the supercritical Froude number is below 1.7 (Henderson 1966). They are caused by channel friction that slows the velocity until any disturbance in the flow generates a spontaneous jump. An undular jump is described by Chanson and Montes (1995) as: "A hydraulic jump of low height [that] is characterized by free-surface undulations downstream of the jump." An undular jump is sometimes preferable because a high tailwater is not required to produce it.

All attempts to create an undular jump in experimental runs failed due to the relatively low submergence ratios and high Froude numbers used in the experiments. However, some experiments had a hydraulic jump form upon initially reaching the corrugations.

Three different situations developed when supercritical flow reached the corrugations, as follows: (1) Flow remained supercritical throughout the corrugations (see Figure 7); (2) Flow went through a hydraulic jump upon initially reaching the corrugations, but returned to supercritical flow after the corrugations (see Figure 8); and (3) Flow went through a hydraulic jump upon initially reaching the corrugations and remained subcritical beyond the corrugations (see Figure 9).

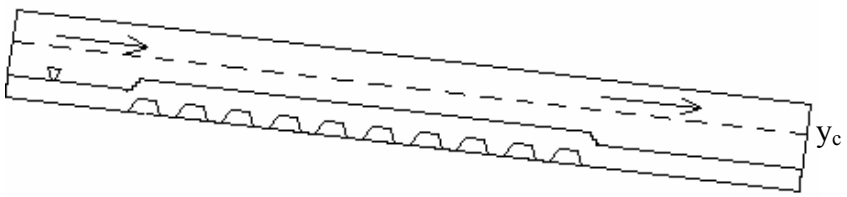

Figure 7. Schematic of Situation 1, flow remaining supercritical throughout corrugations (not to scale).

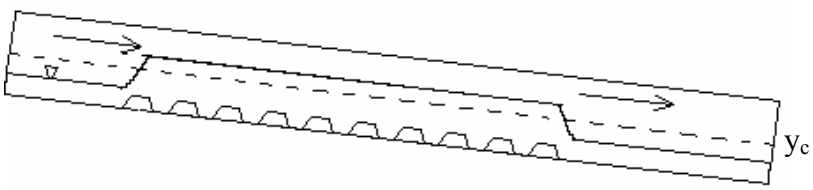

Figure 8. Schematic of Situation 2, flow went through a hydraulic jump upon initially reaching the corrugations and returning to supercritical flow after the corrugations (not to scale).

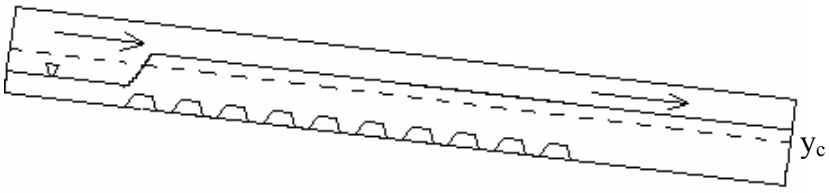

Figure 9. Schematic of Situation 3, flow going through hydraulic jump upon initially reaching the corrugations and remaining subcritical beyond the corrugations (not to scale).

Twenty-seven of the 68 total experiments were run with supercritical flows upstream from the corrugations. Of the 27 experiments, 17 can be described as Situation 1, eight can be described as Situation 2, and two can be described as Situation 3 (see Table 5).

Table 5. Summary of upstream supercritical experiments.

		Upstream		Corrugation		Downstream		
Exp.	Slope	Fr	Depth (m)	Fr	Depth (m)	Fr	Depth (m)	Situation
21	0.021	3.33	0.027	0.75	0.076	0.24	0.158	3
22	0.021	3.87	0.030	0.82	0.088	0.28	0.177	3
23	0.030	3.67	0.018	0.72	0.055	3.67	0.018	2
24	0.030	3.22	0.027	0.86	0.067	4.15	0.024	2
25	0.030	2.93	0.037	0.94	0.082	3.91	0.030	2
26	0.040	3.46	0.018	0.72	0.055	4.16	0.015	2
27	0.040	3.89	0.024	0.95	0.064	5.31	0.021	2
28	0.040	3.81	0.030	1.03	0.076	4.86	0.027	1
29	0.046	3.56	0.018	0.70	0.055	5.48	0.015	2
30	0.046	3.72	0.024	0.86	0.067	5.08	0.021	2
31	0.046	3.81	0.030	1.03	0.076	5.86	0.024	1
32	0.101	5.29	0.046	1.90	0.091	4.33	0.052	1
33	0.101	5.29	0.040	1.68	0.085	5.29	0.040	1
34	0.101	7.15	0.024	1.46	0.076	5.12	0.030	1
35	0.101	4.67	0.024	1.30	0.061	4.67	0.024	1
36	0.080	4.97	0.024	1.23	0.067	4.97	0.024	1
37	0.080	5.24	0.030	1.43	0.079	5.24	0.030	1
38	0.080	4.21	0.046	1.51	0.091	5.30	0.040	1
39	0.080	4.25	0.052	1.56	0.104	5.19	0.046	1
40	0.060	3.71	0.058	1.51	0.107	5.40	0.046	1
41	0.060	4.27	0.046	1.39	0.098	5.01	0.040	1
42	0.060	3.23	0.046	1.31	0.085	4.73	0.034	1
43	0.060	4.77	0.024	1.08	0.070	4.32	0.027	1
44	0.039	4.52	0.024	0.92	0.076	4.52	0.024	2
45	0.039	3.95	0.040	1.14	0.091	3.95	0.040	1
46	0.039	4.25	0.046	1.22	0.107	4.25	0.046	1
47	0.039	4.35	0.052	1.34	0.116	4.35	0.052	1

According to Jain (2001), if a single bump in a channel floor is higher than the critical bump height, flow approaching the bump at supercritical Froude numbers will be forced through a hydraulic jump. A "barrier" Froude number can therefore be calculated for a given discharge where flow with lower Froude numbers when reaching the bump will go through a hydraulic jump and flow with higher Froude numbers when reaching the bump will stay supercritical (see Appendix G for detailed work). For example, given the full-scale prototype with corrugations on

the bottom and sides of a 1.83 meter wide culvert, the "barrier" Froude number can be described in metric units as follows (see Figure 10):

$$Fr_B = 5.86Q^{-0.160} \qquad (6)$$

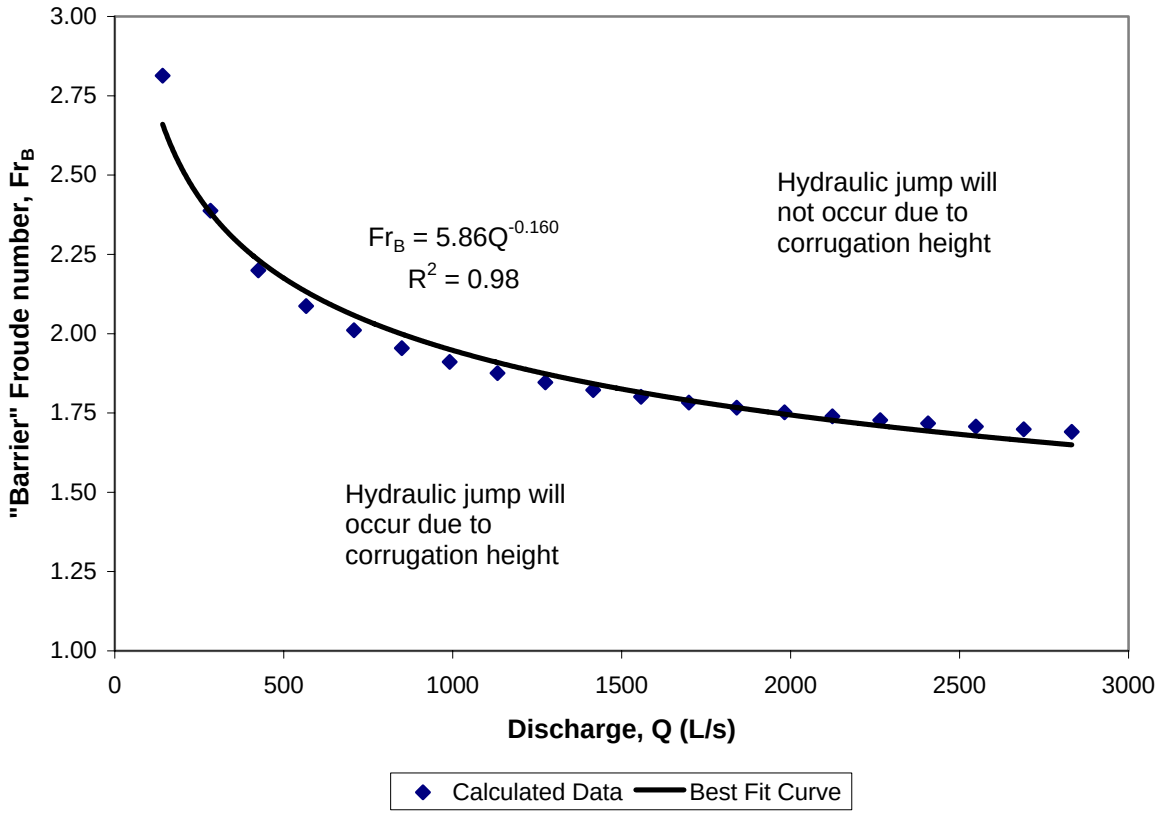

Figure 10. "Barrier" Froude number using 1.83 meter wide culvert with 0.076 meter bottom and side corrugations.

If the data from all three situations are placed on the identical graph, no data points are in the area below the curve (see Figure 11). Therefore, it can be concluded that the hydraulic jumps seen in the experiments are not caused by the height of the corrugation itself. Instead, hydraulic jumps are formed due to the change of the critical slope by the increased roughness.

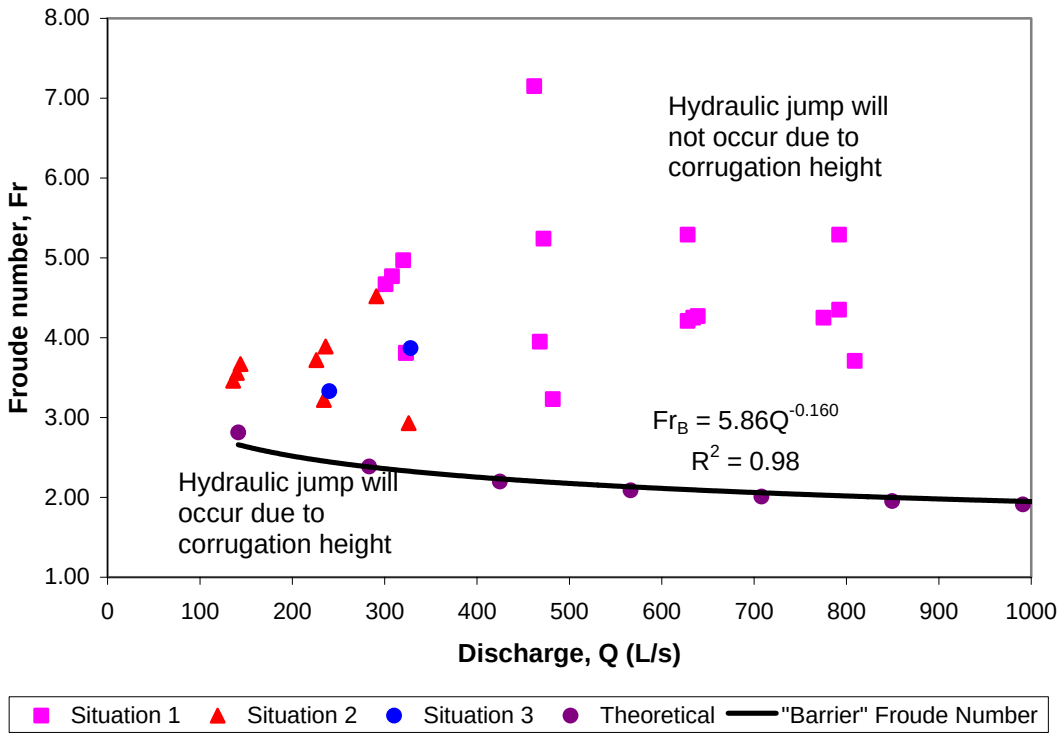

Figure 11. Data of experiments with supercritical flow upstream (scaled to full size) compared to the "Barrier" Froude number.

Hydraulic jumps formed in Situations 2 and 3 because the slope required to produce supercritical flow above the corrugated section of the flume was greater than the actual slope. Hydraulic jumps did not form in Situation 1 because the flume slope was greater than that required to produce supercritical flow above the corrugated section of the flume.

CHAPTER SIX

IMPACT OF INCREASED ROUGHNESS

Impact on Velocity

Although a hydraulic jump did not form in many cases, a significant decrease in velocity was found when comparing upstream and corrugation velocities in upstream supercritical flow conditions (see Figure 12). Decreases in upstream velocities to corrugation velocities range from 44-66 percent in supercritical flow. Using a full size prototype, the percentage decrease in velocity follows a relationship with the dimensionless discharge given by the following equation (see Figure 13):

$$\%decrease = 67 - 0.14Q^* \qquad (7)$$

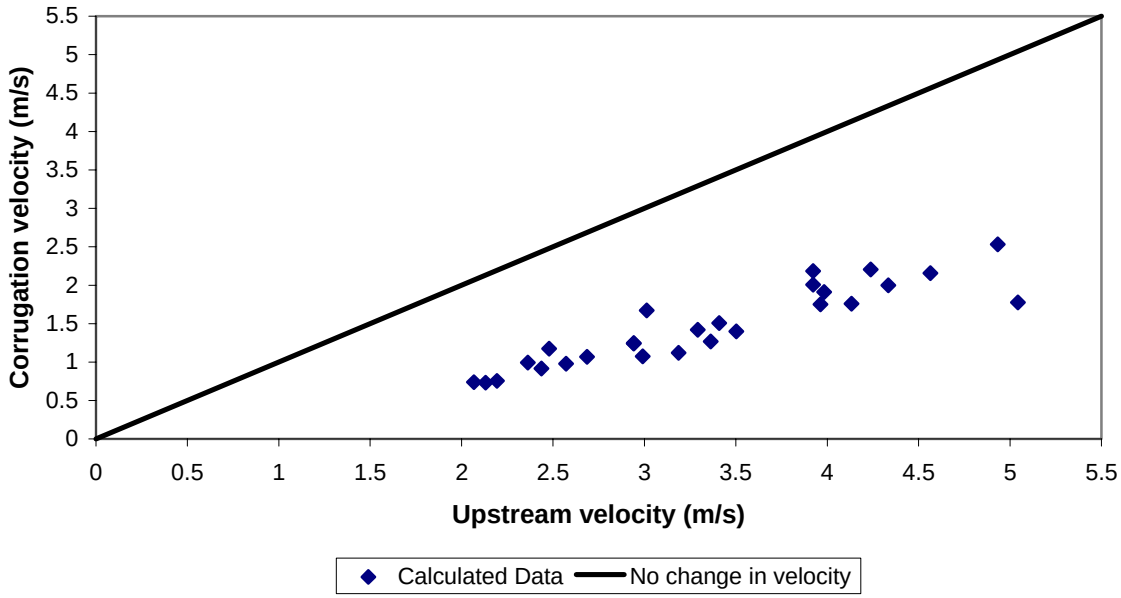

Figure 12. Comparison of corrugation velocity to upstream velocity for supercritical upstream flow conditions on a full size culvert.

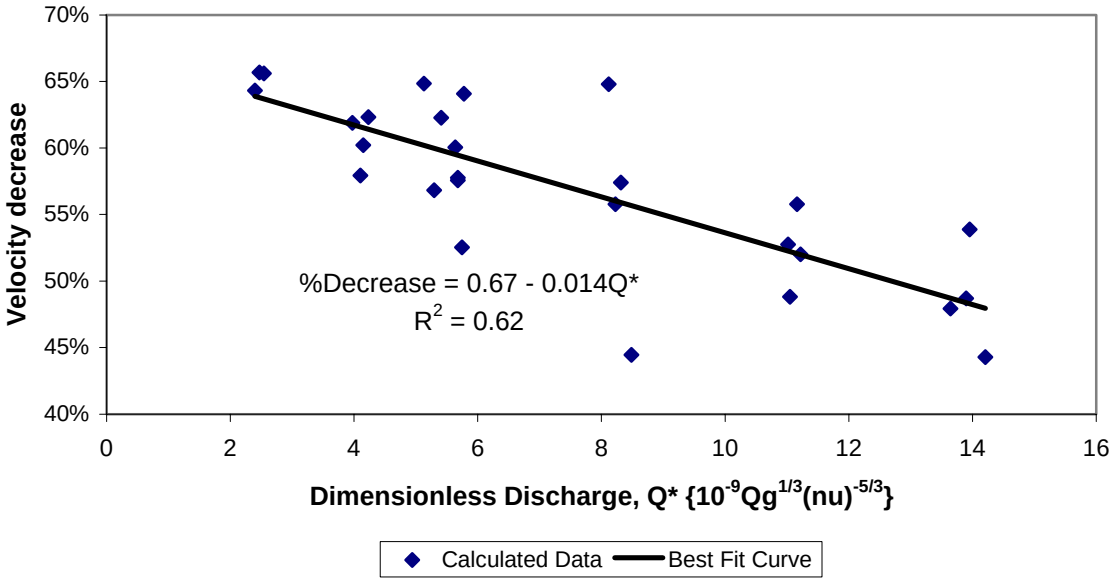

Figure 13. Percentage decrease between upstream velocity and corrugation velocity compared to discharge.

The above relationship is expected due to the decrease in Manning's 'n' when the depth increases. Higher discharge leads to a higher submergence ratio and lower aspect ratio, which lowers the Manning 'n' value from equation (5). A lower Manning 'n' value means less roughness, which means a lesser decrease in velocity.

Impact in a Broken-back Culvert

A broken-back culvert is defined as a culvert that has changes of slope within the culvert barrel. A single broken-back culvert has an initial section of steep slope followed by an outlet section of mild slope (see Figure 14). Due to the steep slope in the initial section, the outlet section has supercritical flow unless a hydraulic jump occurs within the barrel (Hotchkiss et al. 2004).

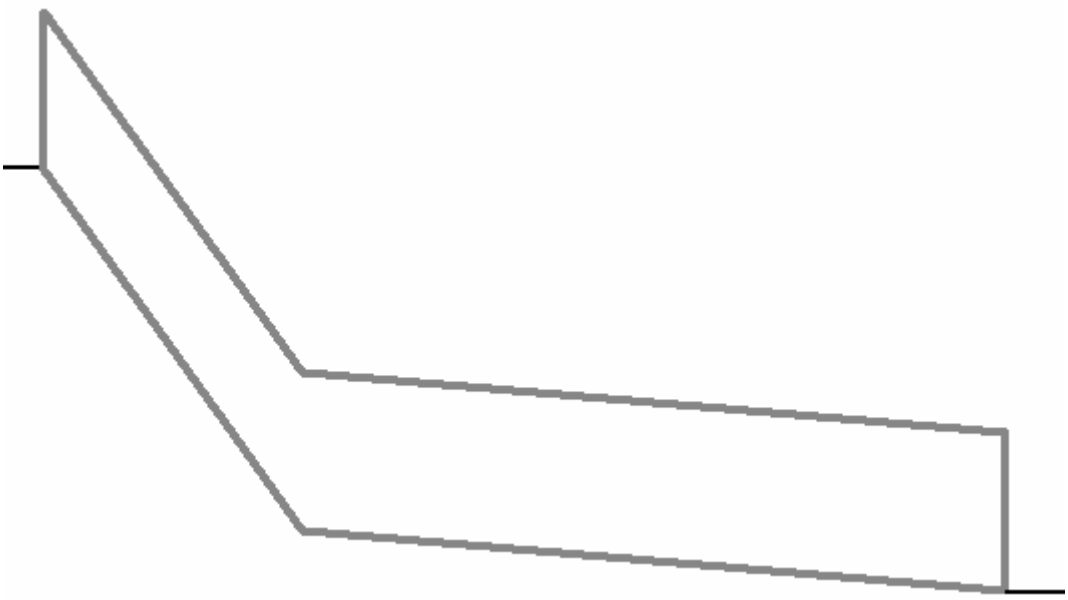

Figure 14. Generic shape of a single broken-back culvert in elevation view. Flow would be from left to right.

As described above, the hydraulic jumps seen in the experiments were caused by increasing the roughness enough that the slope required to maintain supercritical flow was greater than the slope of the flume. In a broken-back culvert, increasing the roughness in the outlet section may increase the slope required to maintain supercritical flow enough that a hydraulic jump will form.

Broken-back culverts can be modeled by the Broken-back Culvert Analysis Program (BCAP). BCAP analyzes the hydraulics of a broken-back culvert using well-known and accepted equations (Hotchkiss et al. 2004). In order to model the proposed corrugations, BCAP outputs must be compared to the experimental results to determine if BCAP can be used as a valid modeler for the corrugations.

The results for three experiments were tested in BCAP to check how the program compared with scaled results. The three experiments corresponded to situations 1, 2, and 3 as described earlier. Experiment 40, where flow remained supercritical throughout (Situation 1),

experiment 27, where a hydraulic jump took place but flow returned to supercritical downstream of the corrugations (Situation 2), and experiment 22, where a hydraulic jump took place (Situation 3), were compared with the outputs of BCAP (see Appendix H for BCAP outputs). Each experiment went through three BCAP tests, as follows (see Table 6): (a) BCAP inputs matched the experimental setup in the tilting flume; (b) Same as (a), except that the initial section's slope was steepened in BCAP so the flow characteristics at the beginning of the outlet section were the same as the experimental flow characteristics; and (c) Same as (b), except that the outlet section's slope was reduced in BCAP until a hydraulic jump was predicted.

Table 6. BCAP setup for testing program to scaled experimental results. Note: Experiments 22 and 27 showed a hydraulic jump on test (b), therefore, test (c) was not necessary.

	Experiment 22		Experiment 27		Experiment 40		
Test	**a**	**b**	**a**	**b**	**a**	**b**	**c**
Experiment Slope	0.021		0.040		0.060		
Discharge (cms)	0.328		0.236		0.806		
Corrugation Manning's 'n'	0.0376		0.0434		0.0347		
Steep section slope	0.021	0.571	0.040	0.790	0.060	0.410	0.410
Outlet section slope	0.021	0.021	0.040	0.040	0.060	0.060	0.025

When comparing BCAP results to experimental results, the most important test to compare is test (b), where the upstream data are similar. If the results from BCAP in the corrugated section are comparable to the actual experimental results, the program can be used as a viable prediction tool in these situations. Because of this, a comparison between BCAP test (b) and experimental results for Measurement 5 was made. Measurement 5 was chosen because its location was at the end of the corrugations and would most likely represent the outlet station in the BCAP program (see Table 7).

Table 7. Comparison of BCAP test (b) outlet predictions to Measurement 5 in tilting flume experiments.

	Experiment 22			Experiment 27			Experiment 40		
	BCAP	**5**	**% Diff.**	**BCAP**	**5**	**% Diff.**	**BCAP**	**5**	**% Diff.**
y (m)	0.15	0.18	-16.7	0.12	0.12	0.0	0.21	0.21	0.0
V (m/s)	1.21	1.07	13.1	1.09	1.11	-1.8	2.18	2.22	-1.8

As shown in Table 7, the depths and velocities predicted by BCAP are relatively close to the experimental results for the test experiments. Based on the comparison of BCAP outputs to the experimental results, BCAP can be reasonably used to predict corrugation data given the flow data upstream.

Furthermore, all 27 experiments with supercritical flow upstream were reproduced in BCAP using test (b). All 17 experiments where a hydraulic jump was not observed (Situation 1) had no hydraulic jump prediction from BCAP, and all ten experiments where a hydraulic jump was observed (Situations 2 and 3) had a hydraulic jump prediction from BCAP. This result further confirms that BCAP can be used to predict corrugation data given the flow data upstream.

For BCAP test (c), the corrugation section required a slope of less than 2.5% to trigger a hydraulic jump in the experiment tested. In most cases, the outlet section of a broken-back culvert is on a zero percent slope. Based on this analysis, it can be assumed that broken-back culverts fitted with the corrugations tested will cause flow to decrease in velocity, creating a hydraulic jump within the culvert in many cases.

CHAPTER SEVEN

VELOCITY PROFILES OVER CORRUGATIONS

Background

Velocity profiles in rough turbulent flow are known to fit the log law. Ead et al. (2000) found this to be the case in corrugated metal pipe (CMP) culverts. The flow was found to fit the Prandtl equation for rough turbulent flow, as follows:

$$\frac{u}{u_*} = \frac{2.30}{\kappa} \log \frac{y_0}{k_s} + 8.50 \qquad (8)$$

where u is the streamwise velocity, u_* is the shear velocity, κ is the von Karman constant (assumed to be 0.40), y_0 is the depth at which the velocity is measured, and k_s is the Nikuradse equivalent sand roughness. Little to no research has been completed on velocity profiles for trapezoidal corrugations.

Purpose

The purpose of this portion of the research was to determine if the velocity profiles in the proposed design of the corrugations within a reinforced concrete box (RCB) culvert fit the log law. The shear velocity and the Nikuradse equivalent sand roughness were compared to the experimental work of Ead et al. (2000).

Experimental Setup

Velocity data were collected in the tilting flume in Albrook Hydraulics Laboratory in the corrugated section at measurement station 3. Data were also collected at measurement station 4 to assure fully developed flow, which was confirmed. Ten trials of varying slopes and discharges were completed (see Table 8). Measurements were taken at the crest and the trough for each experiment. Discharges were collected using a flow meter, slopes were collecting using

a surveying rod and level, and depths were collected using a point gage. Zero depth was defined as halfway between the trough and crest.

Table 8. Summary of slopes, discharges, and water depths for velocity profile experiments.

Experiment #	Slope	Discharge (L/s)	Water Depth (m)
69	0.0188	107	0.125
70	0.0188	152	0.160
71	0.035	161	0.114
72	0.035	77.0	0.091
73	0.002	67.4	0.163
74	0.002	172	0.253
75	0.0095	115	0.149
76	0.0095	57.8	0.105
77	0.031	58.3	0.091
78	0.031	111	0.120

Velocities were collected in the streamwise, transverse, and vertical directions using an Acoustic Doppler Velocimeter (ADV). The ADV was connected to a gantry system above the tilting flume that could be moved in all three dimensions within the flow.

Data were collected at several sample points within the flow field (see Table 9). Data were collected at a rate of 25 samples per second for 120 seconds (3000 samples total) using the Sontek HorizonADV computer program (see Appendix I for raw data). Data were processed using the WinADV computer program to calculate measured velocities within the flow field (Wahl 2000). Those data whose signal-to-noise ratio (SNR) fell below 5dB were discarded according to accepted practice.

Table 9. Summary of collection points in each direction for each velocity profile experiment.

	Measurement 3			*Measurement 3c*		
Experiment #	**Vertical**	**Transverse**	**Total**	**Vertical**	**Transverse**	**Total**
69	3	5	15	2	5	10
70	3	5	15	2	5	10
71	3	5	15	2	5	10
72	3	5	15	2	5	10
73	3	5	15	2	5	10
74	6	5	30	4	5	20
75	13	1	13	13	1	13
76	12	1	12	8	1	8
77	11	1	11	7	1	7
78	11	1	11	9	1	9

Results

Many samples with a low SNR were located close to the water surface. In higher velocities, the flow separates around the stem of the ADV, which creates air bubbles. The air bubbles scatter the signal and cause the SNR to decrease.

Many experimental runs had problems of inconsistent readings from the ADV due to the low SNR. Experiment 75 was found to have consistent data that had a similar slope and discharge when compared with the experimental setup of Ead et al. (2000). For these reasons, the results from this experiment were used to compare against results from Ead et al. (2000).

The streamwise velocity u was found to generally fit a typical log law velocity profile when compared to the vertical depth y_0 (see Figure 15). The streamwise velocity remains mostly negative until approximately 5 cm above the datum, which is 3.1 cm above the corrugation crest. This value is higher than expected, as skimming flow research shows a "pseudo-bottom" at a depth of the step crest, and corrugated culverts have not shown negative velocities. The trapezoidal shape of the corrugations likely has a greater effect on the flow than corrugated

culverts, which is confirmed with the higher Manning 'n' value in the experimental corrugated culverts compared to sinusoidal corrugated culverts.

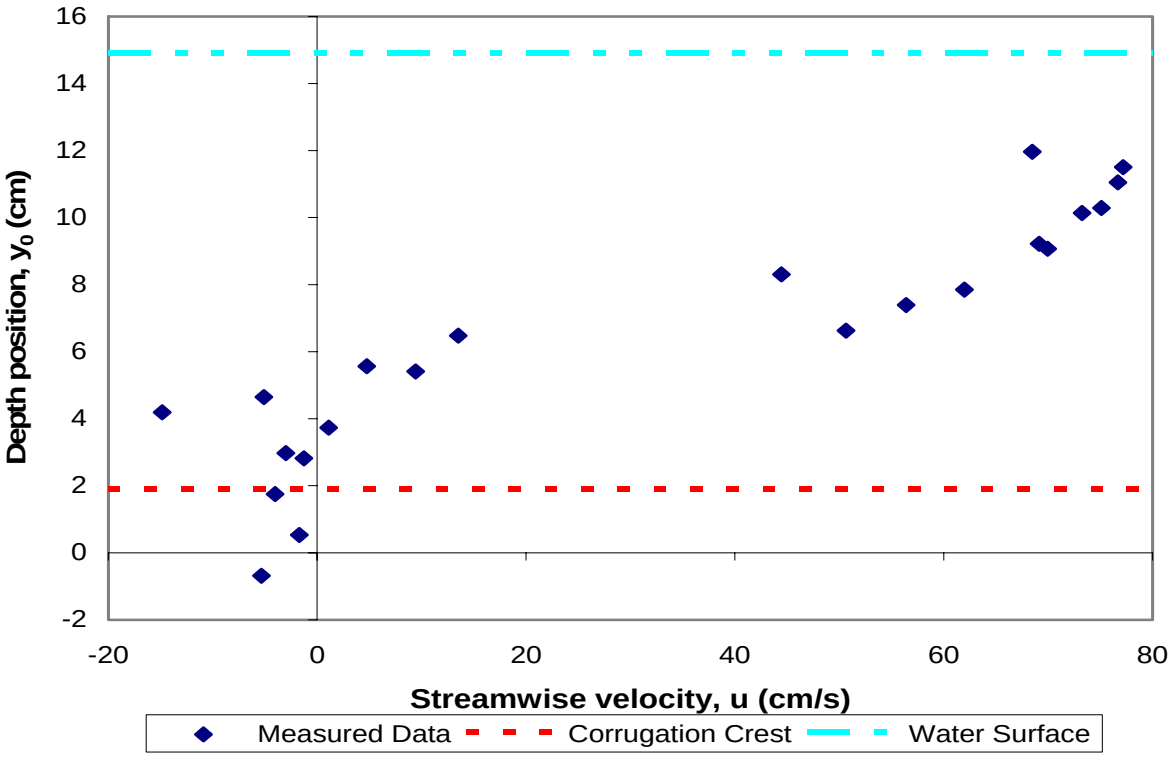

Figure 15. Velocity profile comparing streamwise velocity to depth position for Experiment 75.

In order to determine the shear velocity u_*, the streamwise velocity was plotted against the vertical depth on a semilog scale (see Figure 16). Data points collected at depths below the corrugation crest caused inconsistent results; however, one can use Rotta's method (1962) to shift the reference depth to the top of the corrugation bed and use all data points above the reference depth. Combining this shift with the Prandtl equation (8) gives the following equation, where Δu is the velocity change over the reference shift:

$$\frac{u}{u_*} = \frac{2.30}{\kappa}\log\frac{y_0}{k_s} + 8.50 - \frac{\Delta u}{u_*} \qquad (9)$$

In Experiment 75, Δu is assumed to be 0 because the velocity was not observed to change below the corrugation crest. The shear velocity is the slope of the best fit curve in Figure 16 divided by 5.75 (2.30/κ), as described by Ead et al. (2000). The shear velocity is found to be 28.0 cm/s in Experiment 75.

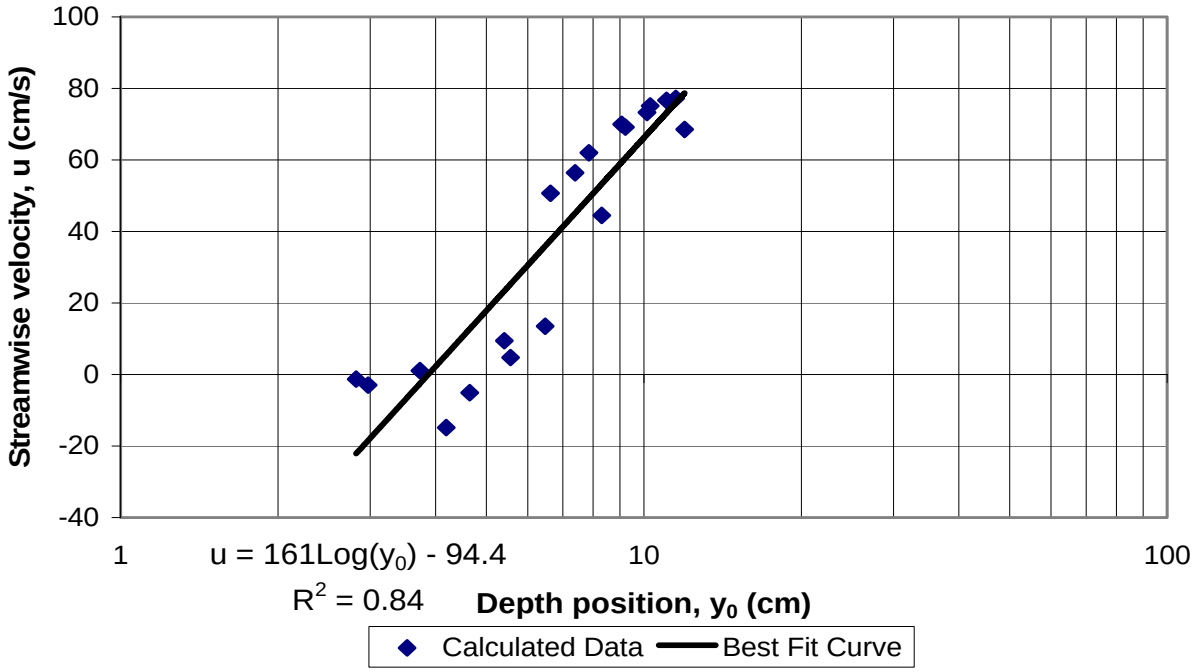

Figure 16. Velocity profile of Experiment 75 used to calculate shear velocity.

The Nikuradse equivalent sand roughness k_s was found using the Prandtl equation (8). Solving for k_s, (8) can be rewritten as:

$$k_s = \frac{y_0}{10^{\frac{\kappa}{2.30}\left(\frac{u}{u_*}-8.5\right)}} \qquad (10)$$

The mean Nikuradse equivalent sand roughness was found to equal 119 cm for Experiment 75. This value is much higher than the amplitude of the corrugations (3.8 cm). While this is unusual, it is possible for values to get this high. Baptist and Mosselman (2002) describe Nikuradse

equivalent sand roughness values of 80 cm for floodplain grassland and 200 cm for ruderal vegetation.

Comparison to Ead et al. (2000)

The above results were compared to results from Ead et al. (2000). The major difference between the experimental setup is the type of corrugations used (see Table 10). As shown, Experiment 75 has corrugations approximately three times larger than that of Ead's experiment 15 in both amplitude and wavelength.

Table 10. Comparison of experimental setup with Ead et al. (2000).

	Experiment 75	**Ead experiment 15**
Culvert type	Modified RCB	CMP
Average width/diameter	Width = 0.86 m	Diameter = 0.622 m
Corrugation amplitude	3.8 cm	1.2 cm
Corrugation wavelength	19.05 cm	6.8 cm
Corrugation type	Trapezoidal	Sinusoidal
Discharge	115 L/s	160 L/s
Slope	0.0095	0.0055

This difference in corrugation amplitude and wavelength should give a similar difference in shear velocity and the Nikuradse equivalent sand roughness. These values were compared with the values from Ead's experiment 15 using both the original and the alternate method of determining shear velocity and the Nikuradse equivalent sand roughness (see Table 11).

Table 11. Comparison of experimental results with Ead et al. (2000).

	Experiment 75	**Ead experiment 15**
Shear velocity u_* (cm/s)	**28.0**	**9.65**
Nikuradse equivalent sand roughness k_s (cm)	**119**	**1.2**

When determining shear velocity and the Nikuradse equivalent sand roughness, the shear velocity is 2.9 times the value of Ead et al. (2000). This is a reasonable value as the Manning roughness coefficient is higher than that of Ead's experiment. A higher roughness leads to a higher shear velocity. It is also reasonable because the amplitude and wavelength are about 3

times higher than that of Ead's experiment. When comparing the Nikuradse equivalent sand roughness, the experimental value is much higher (about 100 times) than that of Ead's experiment. Since the flow can be classified as skimming flow, with recirculating eddies between each corrugation, a high Nikuradse equivalent sand roughness can be expected.

CHAPTER EIGHT

SUMMARY AND CONCLUSIONS

The first objective of this research was to experimentally determine the Manning 'n' value of the proposed corrugations within a RCB culvert. Manning's 'n' was determined to be related by the submergence ratio and aspect ratio, given by equation (5).

The second objective was to attempt to create an undular jump within the experimental flume as expected by BCAP predictions. An undular jump was not observed.

The third objective was to determine the impact the corrugations have on flow conditions, including flow in a broken-back culvert, if the corrugations are applied to the outlet section. Velocities were reduced by 44-66 percent through the corrugations when the upstream section had supercritical flow; this reduction percentage was related to the flow discharge, given by equation (7). BCAP can reasonably be used to predict hydraulic characteristics in a reinforced concrete box culvert with corrugations to increase roughness.

The final objective was to determine if the corrugations follow a log law velocity profile and to compare experimental data with a previously published study on corrugated metal pipe culverts. The shear velocity was found to be 2.9 times that of a study from Ead et al. (2000), and the Nikuradse equivalent sand roughness was found to be approximately 100 times that of the same study. This is expected due to the higher amplitude and wavelength of corrugations.

Based on this research, increased roughness from corrugations will: (1) decrease velocity when encountering supercritical flow, (2) increase the occurrence of hydraulic jumps, and (3) may be an effective means of decreasing the flow energy within a reinforced concrete box

culvert. It is recommended that this design be tested in the field for constructability and to compare field results to experimental results presented in this research.

REFERENCES

Baptist, M. and E. Mosselman (2002). "Biogeomorphological modeling of secondary channels in the Waal River." *River Flow 2002*, Balkena, Lisse, Netherlands.

Boes, R. M. and W. H. Hager (2003). "Hydraulic Design of Stepped Spillways." *Journal of Hydraulic Engineering,* American Society of Civil Engineers, 129(9), 671-679.

"Bridge Flooring" (2006). U.S. Bridge [http://www.usbridge.com/flooring/flspecs.asp], Cambridge, OH.

Chanson, H. and J. S. Montes (1995). "Characteristics of Undular Hydraulic Jumps: Experimental Apparatus and Flow Patterns." *Journal of Hydraulic Engineering*, American Society of Civil Engineers, 121(2), 129-144.

Ead, S. A., N. Rajaratnam, C. Katopodis, and F. Ade (2000). "Turbulent Open-Channel Flow in Circular Corrugated Culverts." *Journal of Hydraulic Engineering.,* American Society of Civil Engineers, 126(10), 750-757.

Henderson, F. M. (1966). *Open Channel Flow,* Macmillan Company, New York.

Hotchkiss, R. H., P. J. Flanagan, and K. Donahoo (2004). "Hydraulics of Broken-back Culverts." *Transportation Research Record 1851,* Transportation Research Board, National Research Council, Washington DC, 35-44.

Hotchkiss, R. H., E. A. Larson, and D. A. Admiraal (2005). "Energy Dissipation in Culverts by Forced Hydraulic Jump Within a Barrel." *Transportation Research Record 1904,* Transportation Research Board, National Research Council, Washington DC, 124-132.

Jain, S. C. (2001). *Open-Channel Flow,* Wiley, New York.

Moore, R. G., P. R. Bedell, and I. D. Moore (1995). "Investigation and Assessment of Long-Span Corrugated Steel Plate Culverts." *Journal of Performance of Constructed Facilities,* American Society of Civil Engineers, 9(2), 85-102.

Ohtsu, I., Y. Yasuda, and M. Takahashi (2004). "Flow Characteristics of Skimming Flows in Stepped Channels." *Journal of Hydraulic Engineering,* American Society of Civil Engineers, 130(9), 860-869.

Pegram, G. G. S., A. K. Officer, and S. R. Mottram (1999). "Hydraulics of Skimming Flow on Modeled Stepped Spillways." *Journal of Hydraulic Engineering,* American Society of Civil Engineers, 125(5), 500-510.

Ring, G. W. (1984). "Culvert Durability: Where Are We?" *Transportation Research Record 1001,* Transportation Research Board, National Research Council, Washington DC, 1-8.

Rotta, J. (1962). "Turbulent boundary layers in incompressible flow." *Progress in Aeronautical Science,* 2, 1-219.

Shafer, J. T. and R. H. Hotchkiss (1998). *Hydraulic Analysis of Broken-back Culverts*. Report SPR-PL-1 33333) P498, Nebraska Department of Roads.

Smith, C. D. (1988). "Flow establishment in helical corrugated pipe." *Canadian Journal of Civil Engineering,* National Research Council Canada, 15, 912-915.

Wahl, T. L. (2000). "Analyzing ADV Data Using WinADV." *2000 Joint Conference on Water Resources Engineering and Water Resources Planning & Management.* Minneapolis, MN.

APPENDIX

APPENDIX A

EXTENDED SKIMMING FLOW LITERATURE SEARCH

Abstract

Stepped spillways have gained interest in hydraulic studies due to the advantages of construction in roller compact concrete dams and greater energy dissipation than that of smooth spillways. Stepped spillways have two main types of flow, nappe flow and skimming flow. Experimental setup includes certain variables such as spillway slope, step height, step length, and critical depth. Different measurement techniques are discussed. Skimming flow is observed to have recirculating flow, water flow with air bubbles, and air flow with water droplets. Equations determining onset of skimming flow, uniform mixture depth, and friction factors are presented. Stepped spillways have a friction factor of 5.5-13 times greater than friction factors of smooth spillways. Stepped spillways also dissipate more than half the energy that would remain at the toe of the spillway if a smooth spillway were installed.

1—Introduction

1.1—Stepped Spillways

1.1.1—Importance

Stepped spillways are an important hydraulic structure used to dissipate energy. Stepped spillways have been used in hydraulic design for over three millennia. By the end of the 1800s, almost one-third of all spillways in North America were of this design. New progress in the 1920s in hydraulic jump energy dissipation characteristics led to the abandonment of stepped spillways, but due to construction techniques such as roller compacted concrete (RCC) dams and

design techniques like embankment protection, stepped spillways have increased in importance since the 1960s [1].

Stepped spillways have two main advantages when compared to smooth spillways. Stepped spillways hold an economical benefit over smooth spillways in RCC dams due to their quick construction time. Stepped spillways also have significant energy dissipation along the spillway because of their "macroroughness," as termed by Boes and Hager (2003). This dissipation of energy reduces the dimensions of stilling basins at the toe of the spillway. Lower flow velocities and high air entrainment reduces the risk of cavitation. A disadvantage to the high air entrainment is that it produces bulking, which increases the required sidewall height [2].

1.1.2—Types of Flow

Two main types of flow exist in stepped spillways. Nappe flow generally occurs on larger steps with small discharges and on relatively mild-sloped spillways [3]. Nappe flow is described as having an air pocket at each step [4]. Nappe flow is also known as jet flow [5]. A sketch of nappe flow is shown in Figure A-1.

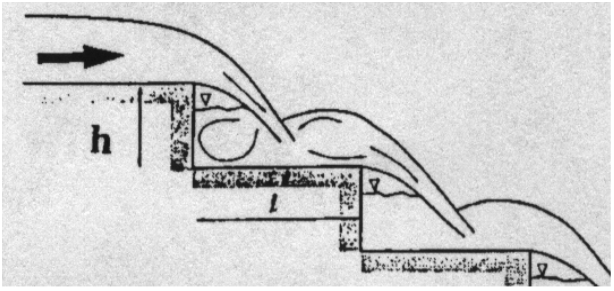

Figure A-1. Sketch of nappe flow [6]

Skimming flow generally occurs on steep-sloped spillways with small steps relative to the water depth [3]. Skimming flow is described as having a so-called "pseduo-bottom" along the step edges with circulating eddies formed at each step [4]. A sketch of skimming flow is shown in Figure A-2.

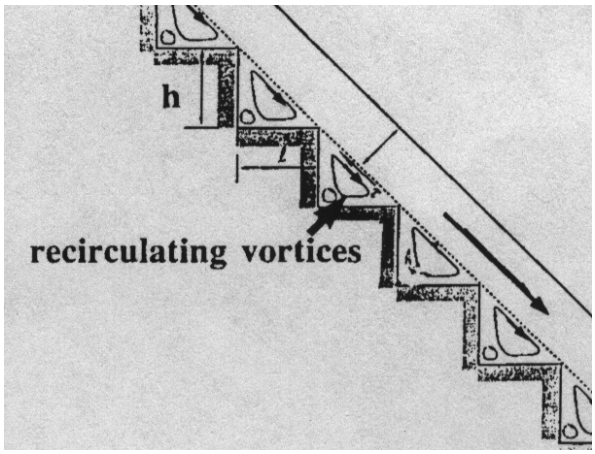

Figure A-2. Sketch of skimming flow [6]

There is some debate about whether a third type of flow exists between nappe flow and skimming flow. Some publications describe transition flow as a separate flow where qualities of both nappe flow and skimming flow exist. Ohtsu, Yasuda, and Takahashi describe transition flow as "flow in which a nappe with an air pocket is not always formed and corner eddies are partly formed at some steps" [4].

1.2—Purpose

The purpose of this appendix is to explore characteristics of skimming flow in stepped spillways from previous work. Typical experimental methods of previous publications will be described, results from selected recent published experiments will be presented, and conclusions from these experiments will be discussed.

2—Methods

2.1—Experimental Setup

Although several details regarding the experimental setup are different among studied publications, all have the same general characteristics. All experiments use a stepped channel with a slope of some constant ϕ, a constant step height h (also denoted as s), a constant step length l, and a critical depth y_c (also denoted as h_c) [2]. Typical variables are shown in Figure A-

3. A sketch of a typical laboratory setup is shown in Figure A-4, and a photograph of this setup is shown in Figure A-5. Experiments generally vary the setup characteristics to create a broad range of situations that the experimental results are valid [4]. See Table A-1 for an example of experimental conditions used in one of the experiments.

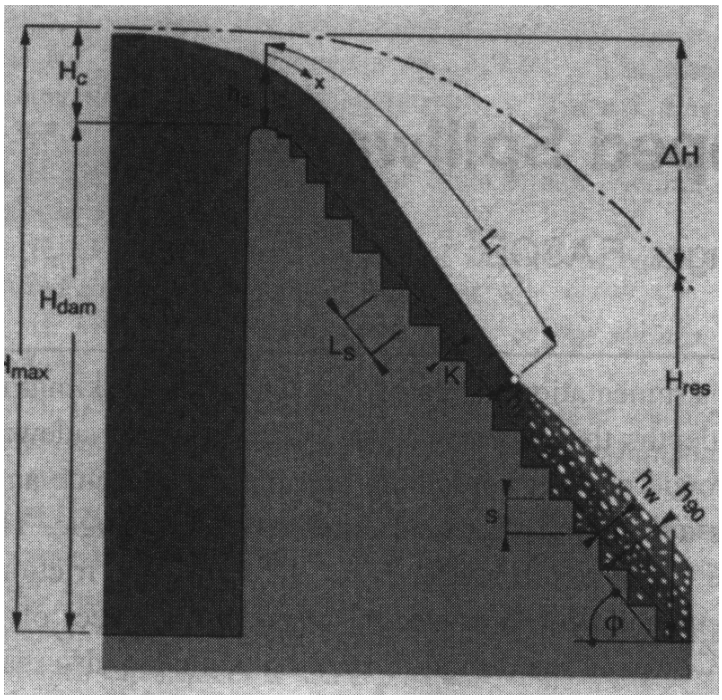

Figure A-3. Typical variables [2] (Note: not all variables shown above are described in this appendix)

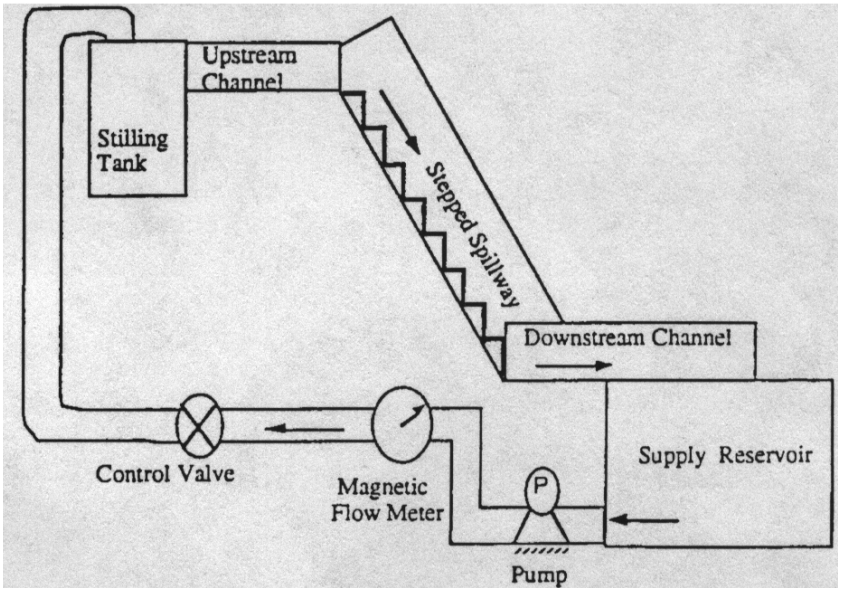

Figure A-4: Sketch of experimental setup [6]

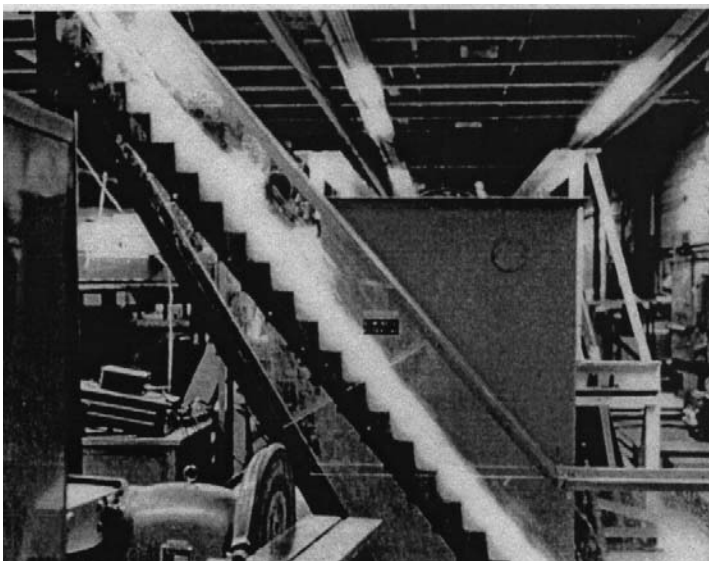

Figure A-5: Photograph of experimental setup [5]

Table A-1: Experimental conditions [4]

θ (deg)	H_{dam}/d_c	S/d_c	$R\times10^{-4}$	$W\times10^{-2}$	S (cm)	H_{dam} (cm)
5.7	2.0–38.5	0.07–0.80	2.2–8.0	3.5–27	0.625–5.0	30–70
8.53	9.8–22.6	0.09–0.81	2.4–5.3	4.2–14	0.625–5.0	65
11.3	3.8–19.0	0.07–0.68	2.2–8.3	3.7–27	0.625–5.0	30–70
19	6.3–47.7	0.02–0.91	2.2–8.6	4.4–35	0.625–5.0	58–240
23	21.4–43.7	0.10–1.00	2.0–6.0	4.3–20	0.625–5.0	153
30	6.4–60.1	0.05–0.99	2.2–8.6	4.6–55	0.625–5.0	59–153
55	6.5–82.4	0.03–1.21	1.6–9.3	4.8–52	0.625–10.0	45–247

2.2—Experimental Measurement Techniques

Publications studied present various methods of taking measurements for their experiments. Ohtsu, Yasuda, and Takahashi measure water discharge with a sharp-edge weir, water depths with a point gage, and air concentration with an electrical void probe [4]. Boes and Hager use a two-tip fiber optical probe to measure air concentration and flow velocity [2]. Chamani and Rajaratnam use a magnetic flow meter to measure the discharge and a Prandtl tube to measure velocity. Chamani and Rajaratnam also use a high-speed video camera to record visual observations in their experiment [5].

3—Results

3.1—Observational Results

Observations from experimental work are not as useful in written publications; however, they serve an important purpose to the reader. Much of the description of skimming flow is embedded in the definition itself, but some publications go into more detail.

Pegram, Officer, and Mottram observe skimming flow as "moving down the spillway almost without touching the steps" and a vortex of rotating aerated water in the space between steps [3]. A sketch from their publication is shown in Figure A-6.

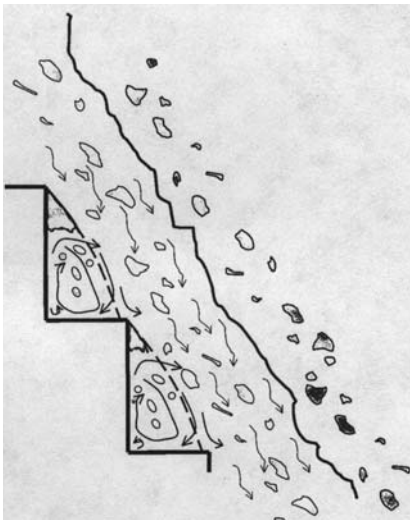

Figure A-6: Sketch of skimming flow [3]

Chamani and Rajaratnam describe flow in their experiment as being "self-aerated, with the air bubbles penetrating to the bottom of the channel." Chamani and Rajaratnam also observe two regions, also referred to as phases, where air bubbles travel in water flows in the lower region and water drops travel in air flow in the upper region [5]. Pegram, Officer, and Mottram also mention this phenomenon, although they do not describe it in detail [3]. A photograph included in the publication by Chamani and Rajaratnam is shown in Figure A-7.

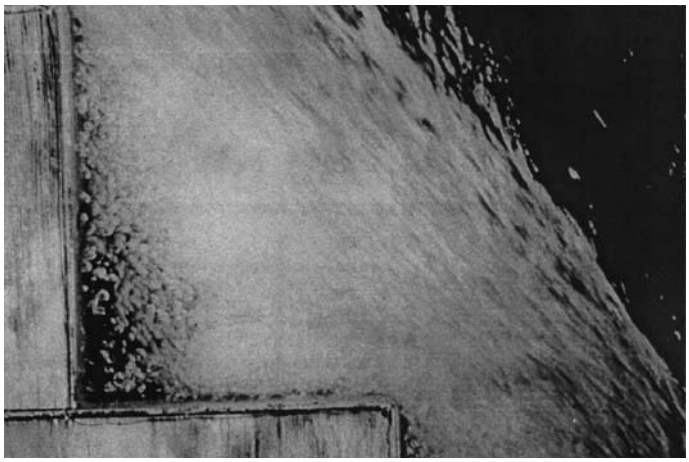

Figure A-7: Photograph of skimming flow [5]

3.2—Numerical Results

The majority of results in publications studied are numerical. Although all publications create equation and figures from their results, the only publication studied that includes a tabular form of initial results is the experiment of Chamani and Rajaratnam. This table, which shows typical data collected for skimming flow experiments, is shown in Table A-2.

Table A-2: Initial Results of Experiment [5]

l/h (1)	h (mm) (2)	Q (L/s) 3)	y_c/h (4)	y_T (mm) (5)	y_m (mm) (6)	$y_T + y_m$ (mm) (7)	$y_{0.9}$ (mm) (8)	$(y_T + y_m)/y_{0.9}$ (9)	y_{um} (mm) (10)	y_{um}/y_T (11)	C (%) (12)	C_T (%) (13)	u_* (m/s) (14)
0.6	125	24.32	0.7	—	—	—	53	—	57	—	53.3	—	1.02
		29.71	0.8	33	31.8	64.8	62.3	1.04	57	1.73	50.8	53	0.85
		41.53	1	42	30.8	72.8	72	1.01	69	1.64	44.8	50	0.97
		47.91	1.1	51	29.6	80.6	79.2	1.02	66	1.29	41.4	52	0.9
		54.59	1.2	60	30.8	90.8	92	0.99	69	1.15	42	54.5	0.82
		61.55	1.3	69	25.5	94.5	99	0.95	69	1.00	40.1	58.5	0.8
0.6	62.50	21.76	1.3	36	16.4	52.4	49	1.07	36	1.00	55.5	71	0.64
		24.32	1.4	39	21	60	55	1.09	39	1.00	55.8	69	0.65
		26.97	1.5	42	20	62	59.3	1.05	45	1.07	53.6	67.5	0.63
		29.71	1.6	45	26.2	71.2	62	1.15	45	1.00	51	69	0.7
		32.54	1.7	45	26.3	71.3	63	1.13	45	1.00	49.7	65	0.75
		35.46	1.8	45	25.6	70.6	65.1	1.08	45	1.00	47.4	60	0.76
		41.53	2	48	28.3	76.3	75	1.02	60	1.25	46.8	54	0.71
		44.68	2.1	51	29.8	80.8	76.5	1.06	63	1.24	45.4	56	0.79
		47.91	2.2	54	22.7	76.7	79	0.97	66	1.22	43.1	53	0.72
		51.21	2.3	57	27.1	84.1	81	1.04	69	1.21	41.8	56	0.74
		54.59	2.4	60	25.2	85.2	83.4	1.02	66	1.10	41.2	59	0.75
		58.03	2.5	63	22.9	85.9	86.4	0.99	63	1.00	40.1	60	0.73
		61.55	2.6	66	22.9	88.9	92	0.97	66	1.00	39	60	0.73
0.6	31.25	21.76	2.6	30	19.5	49.5	48	1.03	39	1.30	51.3	54.2	0.73
		24.32	2.8	39	16.2	55.2	53.2	1.04	39	1.00	49.4	64.2	0.68
		26.97	3	42	16	58	55.8	1.04	42	1.00	48	65.4	0.67
		29.71	3.2	45	15.7	60.7	58.9	1.03	48	1.07	48	68.5	0.68
		32.54	3.4	45	17.3	62.3	61.7	1.01	48	1.07	45.7	61.6	0.67
		35.46	3.6	45	21.4	66.4	64.9	1.02	51	1.13	45.1	58.6	0.67
		38.45	3.8	45	23.5	68.5	69	0.99	48	1.07	45.4	54.7	0.69
		41.53	4	48	21.3	69.3	69.4	1.00	51	1.06	43	55.8	0.68
		44.68	4.2	51	20.1	71.1	71.4	1.00	54	1.06	40.4	55.2	0.66
		47.91	4.4	51	24.2	75.2	74.3	1.01	54	1.06	39.1	50.7	0.65
0.8	125	29.71	0.8	36	28.9	64.9	64.5	1.01	42	1.17	48.5	52.3	0.95
		35.46	0.9	45	30.2	75.2	72.4	1.04	60	1.33	47.2	56.5	0.91
		41.53	1	51	29.5	80.5	83.8	0.96	60	1.18	47	56.5	0.93
		47.91	1.1	60	26.1	86.1	91.3	0.94	66	1.10	45.7	61.2	0.88
		54.59	1.2	66	28.2	94.2	95.6	0.99	66	1.00	42.6	60.8	0.9
		61.55	1.3	69	24	93	103.5	0.90	72	1.04	42.7	56.9	0.95
0.8	31.3	21.76	2.6	24	23.5	47.5	45.7	1.04	36	1.50	52.6	48.8	0.87
		24.32	2.8	30	18.4	48.4	49.1	0.99	39	1.30	52.4	54.6	0.83
		26.97	3	30	22.8	52.8	52.7	1.00	42	1.40	51.3	50.2	0.82
		29.71	3.2	33	21.3	54.3	55.7	0.97	45	1.36	50.5	52.7	0.82
		32.54	3.4	36	20.6	56.6	58	0.98	51	1.42	47.3	54.5	0.80
		35.46	3.6	39	23.7	62.7	61.3	1.02	54	1.38	48.8	54.5	0.78
		38.45	3.8	39	25.3	64.3	63.5	1.01	54	1.38	47.7	51.3	0.80
		41.53	4	39	26.8	65.8	65	1.01	60	1.54	44.8	48.5	0.82
		44.68	4.2	42	26.5	68.5	68.1	1.01	72	1.71	46.9	48.6	0.82
		47.91	4.4	45	26	71	70.1	1.01	57	1.27	46.5	49.6	0.77

3.2.1—Formation of Skimming Flow

Extensive research attempts to find an equation that determines the situation at which skimming flow occurs has been done. Chamani and Rajaratnam determine that skimming flow formation depends on the step height, step length, and critical depth in the following equation [6]:

$$\frac{h}{l} = \sqrt{0.89[(\frac{y_c}{h})^{-1} - (\frac{y_c}{h})^{-0.34} + 1.5] - 1} \qquad \text{(A-1)}$$

Boes and Hager determine the transition between skimming flow and nappe flow to be dependent on critical depth, step height, and spillway slope in the equation [2]:

$$\frac{y_c}{h} = 0.91 - 0.14\tan\phi \qquad \text{(A-2)}$$

3.2.2—Uniform Mixture Depth

The uniform mixture depth, y_{90}, is the depth where the air concentration equals 0.9. This depth is important in that it determines the sidewall height for design purposes [2]. It is also important in that many experiments studied used this value as an upper limit for determining properties such as flow velocity and air concentration. Boes and Hager determine the uniform mixture depth to fit the following equation [2]:

$$\frac{y_{90}}{h} = 0.50F_*^{0.1\tan\phi+0.5} \qquad \text{(A-3)}$$

3.2.3—Friction

Many publications discuss friction in the results of their experiments. Chamani and Rajaratnam give friction in terms of a skin friction coefficient, c_f, which is found to be a function of the uniform mixture depth and of the roughness height, as shown in the following equation [5]:

$$\frac{1}{\sqrt{c_f}} = 3.85\log(\frac{y_{90}}{k}) + 3.53 \qquad \text{(A-4)}$$

Boes and Hager determine the friction factor to be a function of roughness height, channel slope, and hydraulic diameter. They present the following equation [2]:

$$f_b = [0.5 - 0.42\sin(2\phi)](\frac{k}{D_h})^{0.2} \qquad \text{(A-5)}$$

Ohtsu, Yasuda, and Takahashi find the friction factor in a stepped channel to be anywhere from 5.5 to 13 times that of a smooth channel with similar slope and material [4].

3.2.4—Energy

Energy is of major importance in studied publications, as energy dissipation is one of the major advantages to having a stepped spillway compared to a smooth spillway. Pegram, Officer, and Mottram describe the energy dissipation ratio (EDR) as [3]:

$$EDR = \frac{E_{smooth} - E_{stepped}}{E_{smooth}} \qquad \text{(A-6)}$$

They find the EDR to be 54-60% when the spillway is at equilibrium, which is higher than previous works that predicted the EDR at 89% [3]. Chamani and Rajaratnam agree with the above results, as they find the EDR to be 48-63% [5].

4—Discussion

From the above results, it is important to realize that different experiments create different equations, even though the experiments are testing a similar situation. In the formation of skimming flow, one is tempted to use the equation formed by Boes and Hager due to its simplicity; however, one must review the original publication to determine if the equation is valid for the situation for which it will be applied. In order to create equations valid for a wide range of situations, previous work should be compiled and added to additional experiments and full-scale models.

It is interesting to note that Chamani and Rajaratnam is the only publication researched that included both a descriptive analysis and a sketch of their experimental setup. This makes the experiment more easily replicable than those that only give a description (Pegram, Officer, and Mottram) or those that refer to other publications to describe their experimental setup (Boes and Hager).

5—Conclusion

Skimming flow in stepped spillways is unique in that it has three unique phases of flow: recirculating flow in a vortex in between spillway steps, water with air bubbles skimming over the spillway steps, and water droplets in an air flow above the water flow. Skimming flow properties are dependent on the spillway slope, the critical depth, the step height and the step length. The spillway slope has a greater effect on friction factors compared to the roughness. Energy dissipation is much greater in stepped spillways compared to smooth spillways; usually, a stepped spillway in skimming flow situations dissipates more than half the energy that would have been at the toe of a smooth spillway. There is no equation that is "better" than another in these cases studied; instead, one should refer to the original publications to determine which equations are valid for each situation. Compilation of previous work, additional experimental tests, and testing on full-scale models are necessary to produce an equation that can be used in a wide variety of situations.

6—Notation

The following symbols are used in this appendix:

c_f = skin friction coefficient

D_h = hydraulic diameter (4 times the hydraulic radius)

EDR = energy dissipation ratio

E_{smooth} = specific energy at toe of smooth spillway

$E_{stepped}$ = specific energy at toe of stepped spillway

F_* = roughness Froude number $[q/(g \sin \phi h^3)^{1/2}]$

f_b = friction factor of bottom roughness

h = step height

k = roughness height $[hl/(h^2 + l^2)^{1/2}]$

l = step length

y_c = critical depth

y_{90} = uniform mixture depth

ϕ = spillway slope

7—References

[1] Chanson, H. "Hydraulic Engineering into the 21st Century: a Rediscovery of the Wheel? 2 New Challenges." Proc. 6th International Conference on Civil Engineering. Isfahan, Iran: 2003.

[2] Boes, R. M. and W. H. Hager. "Hydraulic Design of Stepped Spillways." Journal of Hydraulic Engineering 129 (2003): 671-679.

[3] Pegram, G. G. S., A. K. Officer, and S. R. Mottram. "Hydraulics of Skimming Flow on Modeled Stepped Spillways." Journal of Hydraulic Engineering 125 (1999): 500-510

[4] Ohtsu, I., Y. Yasuda, and M. Takahashi. "Flow Characteristics of Skimming Flows in Stepped Channels." Journal of Hydraulic Engineering 130 (2004): 860-869.

[5] Chamani, M. R. and N. Rajaratnam. "Characteristics of Skimming Flow over Stepped Spillways." Journal of Hydraulic Engineering 125 (1999): 361-368.

[6] Chamani, M. R. and N. Rajaratnam. "Onset of Skimming Flow on Stepped Spillways." Journal of Hydraulic Engineering 125 (1999): 969-971.

APPENDIX B

RAW DATA

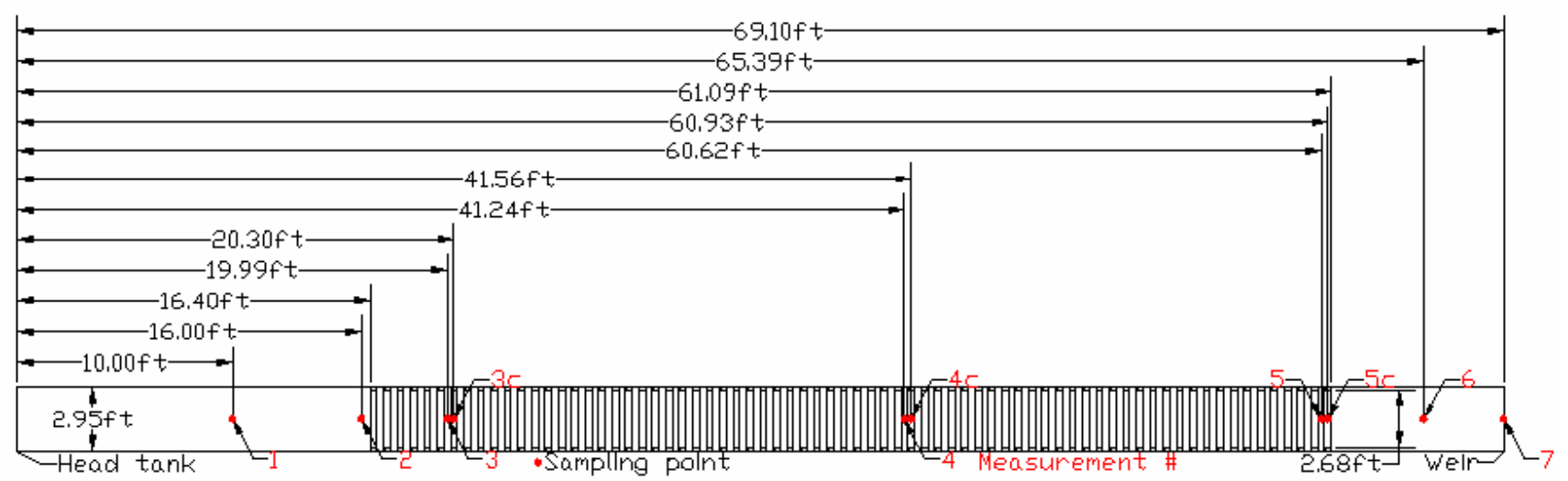

Figure B-1. Location of measurement points in tilting flume.

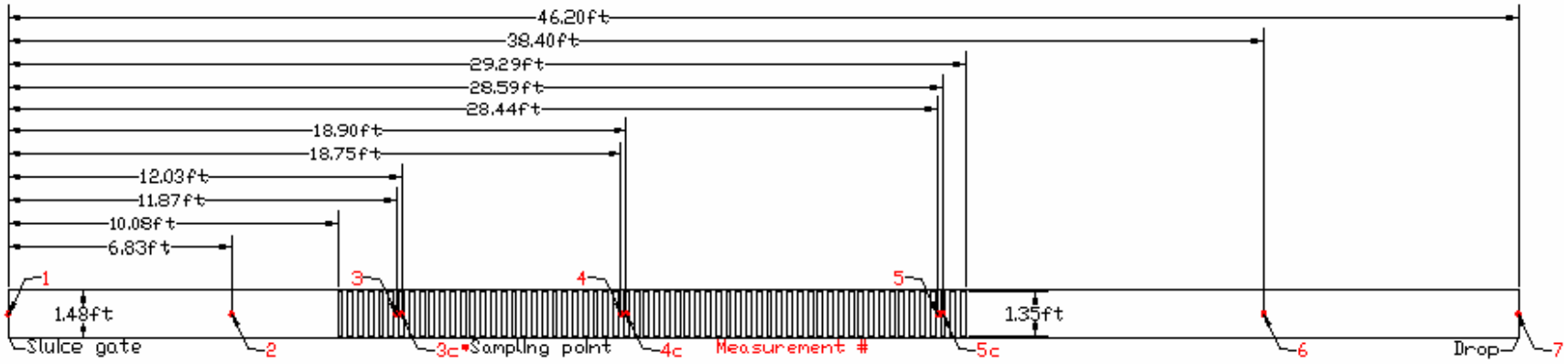

Figure B-2. Location of measurement points in Sloan flume.

Table B-1. Slope and point gage readings for channel bottom for tilting flume (in feet). Measurements 1 and 2 did not have any point gage readings because the gantry system did not go to those points. Other entries may not have point gage readings due to high slopes.

		Measurement number							
Experiment	**Slope**	**3**	**3c**	**4**	**4c**	**5**	**5c**	**6**	**7**
1	0.0028	0.307	0.434	0.236	0.363	0.164	0.291	0.104	0.345
2	0.0028	0.307	0.434	0.236	0.363	0.164	0.291	0.104	0.343
3	0.0028	0.307	0.434	0.236	0.363	0.164	0.291	0.104	0.373
4	0.006	0.402	0.527	0.267	0.394	0.138	0.263	0.063	0.271
5	0.006	0.402	0.527	0.267	0.394	0.138	0.263	0.063	0.303
6	0.006	0.402	0.527	0.267	0.394	0.138	0.263	0.063	0.272
7	0.006	0.402	0.527	0.267	0.394	0.138	0.263	0.063	0.302
8	0.009	0.496	0.619	0.298	0.423	0.112	0.237	0.023	0.234
9	0.009	0.496	0.619	0.298	0.423	0.112	0.237	0.023	0.232
10	0.009	0.496	0.619	0.298	0.423	0.112	0.237	0.023	0.232
11	0.0118	0.682	0.805	0.422	0.546	0.179	0.303	0.075	0.287
12	0.0118	0.682	0.805	0.422	0.546	0.179	0.303	0.075	0.284
13	0.0118	0.682	0.805	0.422	0.546	0.179	0.303	0.075	0.283
14	0.015	0.777	0.898	0.453	0.574	0.152	0.274	0.033	0.241
15	0.015	0.777	0.898	0.453	0.574	0.152	0.274	0.033	0.242
16	0.015	0.777	0.898	0.453	0.574	0.152	0.274	0.033	0.242
17	0.0183	0.947	1.069	0.552	0.674	0.185	0.306	0.049	0.288
18	0.0183	0.947	1.069	0.552	0.674	0.185	0.306	0.049	0.259
19	0.0183	0.947	1.069	0.552	0.674	0.185	0.306	0.049	0.288
20	0.021	1.109	1.229	0.656	0.778	0.237	0.358	0.087	0.327
21	0.021	1.109	1.229	0.656	0.778	0.237	0.358	0.087	0.328
22	0.021	1.109	1.229	0.656	0.778	0.237	0.358	0.087	0.326
23	0.03	1.548	1.665	0.905	1.024	0.314	0.431	0.119	0.024
24	0.03	1.548	1.665	0.905	1.024	0.314	0.431	0.119	0.024
25	0.03	1.548	1.665	0.905	1.024	0.314	0.431	0.119	0.024
26	0.04	-	-	1.191	1.307	0.399	0.513	0.152	0.021
27	0.04	-	-	1.191	1.307	0.399	0.513	0.152	0.021
28	0.04	-	-	1.191	1.307	0.399	0.513	0.152	0.021
29	0.0463	-	-	1.507	1.671	0.647	0.756	0.371	0.218
30	0.0463	-	-	1.507	1.671	0.647	0.756	0.371	0.218
31	0.0463	-	-	1.507	1.671	0.647	0.756	0.371	0.218
32	0.1008	-	-	-	-	0.009	0.103	-	-
33	0.1008	-	-	-	-	0.009	0.103	-	-
34	0.1008	-	-	1.973	2.071	0.009	0.103	-	-
35	0.1008	-	-	1.973	2.071	0.009	0.103	-	-
36	0.08	-	-	1.571	1.674	0.003	0.105	-	-
37	0.08	-	-	1.571	1.674	0.003	0.105	-	-
38	0.08	-	-	1.571	1.674	0.003	0.105	-	-
39	0.08	-	-	1.571	1.674	0.003	0.105	-	-
40	0.06	-	-	1.726	1.835	0.55	0.659	0.202	0.005
41	0.06	-	-	1.726	1.835	0.55	0.659	0.202	0.005
42	0.06	-	-	1.726	1.835	0.55	0.659	0.202	0.005

Table B-1 (continued).

		Measurement number							
Experiment	**Slope**	**3**	**3c**	**4**	**4c**	**5**	**5c**	**6**	**7**
43	0.06	-	-	1.726	1.835	0.55	0.659	0.202	0.005
44	0.0388	1.603	1.713	0.768	0.884	0.005	0.119	-	-
45	0.0388	1.603	1.713	0.768	0.884	0.005	0.119	-	-
46	0.0388	1.603	1.713	0.768	0.884	0.005	0.119	-	-
47	0.0388	1.603	1.713	0.768	0.884	0.005	0.119	-	-
48	0.0235	1.22	1.339	0.71	0.832	0.243	0.363	0.079	0.003
49	0.0235	1.22	1.339	0.71	0.832	0.243	0.363	0.079	0.003
50	0.0235	1.22	1.339	0.71	0.832	0.243	0.363	0.079	0.003

Table B-2. Point gage reading for water level for tilting flume (in feet). In cases where the point gage was unable to reach the measurement point, the data is the actual water depth, taken by a ruler. In some cases, measurement 2 does not have data due to the high variability in depths at the measurement point.

	Measurement number									
Experiment	**1**	**2**	**3**	**3c**	**4**	**4c**	**5**	**5c**	**6**	**7**
1	0.42	0.44	0.695	0.693	0.615	0.613	0.540	0.538	0.551	0.520
2	0.49	0.52	0.758	0.760	0.683	0.681	0.603	0.601	0.623	0.586
3	0.58	0.60	0.841	0.841	0.768	0.770	0.701	0.699	0.721	0.676
4	0.35	0.39	0.719	0.731	0.593	0.593	0.459	0.453	0.476	0.448
5	0.43	0.47	0.808	0.784	0.668	0.664	0.562	0.561	0.584	0.550
6	0.43	0.47	0.807	0.782	0.663	0.661	0.519	0.515	0.550	0.518
7	0.50	0.54	0.864	0.843	0.731	0.728	0.609	0.613	0.646	0.601
8	0.31	0.36	0.794	0.792	0.603	0.601	0.417	0.412	0.438	0.403
9	0.39	0.45	0.846	0.856	0.664	0.661	0.474	0.471	0.509	0.474
10	0.46	0.52	0.915	0.917	0.716	0.714	0.525	0.521	0.567	0.536
11	0.28	0.36	0.975	0.975	0.709	0.703	0.460	0.460	0.488	0.462
12	0.37	0.43	1.027	1.020	0.762	0.762	0.518	0.514	0.557	0.529
13	0.43	0.50	1.069	1.064	0.811	0.811	0.562	0.551	0.609	0.583
14	0.24	0.34	1.049	1.047	0.726	0.721	0.414	0.411	0.435	0.412
15	0.33	0.43	1.108	1.105	0.778	0.775	0.473	0.466	0.513	0.487
16	0.39	0.50	1.165	1.153	0.829	0.829	0.517	0.510	0.576	0.545
17	0.22	0.34	1.222	1.219	0.826	0.818	0.467	0.459	0.495	0.466
18	0.28	0.40	1.267	1.261	0.866	0.863	0.490	0.481	0.528	0.506
19	0.30	0.48	1.318	1.306	0.911	0.911	0.563	0.563	0.627	0.594
20	0.18	0.31	1.372	1.372	0.919	0.914	0.505	0.497	0.531	0.507
21	0.09	0.36	1.423	1.418	0.966	0.957	0.554	0.551	0.606	0.573
22	0.10	0.44	1.466	1.461	1.004	1.004	0.591	0.591	0.664	0.636
23	0.06	0.26	1.796	1.792	1.151	1.144	0.559	0.542	0.179	0.099
24	0.09	0.33	1.839	1.834	1.197	1.187	0.597	0.578	0.195	0.128
25	0.12	0.40	1.890	1.880	1.235	1.228	0.633	0.611	0.218	0.153
26	0.06	0.23	0.250	0.130	1.425	1.416	0.629	0.617	0.205	0.096
27	0.08	0.28	0.290	0.140	1.469	1.456	0.668	0.651	0.217	0.130
28	0.10	0.09	0.330	0.180	1.504	1.487	0.705	0.686	0.237	0.155
29	0.06	0.21	0.250	0.120	1.790	1.777	0.884	0.859	0.416	0.296
30	0.08	0.06	0.290	0.170	1.824	1.812	0.911	0.894	0.436	0.332

Table B-2 (continued).

	Measurement number									
Experiment	**1**	**2**	**3**	**3c**	**4**	**4c**	**5**	**5c**	**6**	**7**
31	0.10	0.08	0.310	0.180	1.864	1.847	0.943	0.926	0.446	0.336
32	0.15	-	0.354	0.229	0.375	0.229	0.389	0.323	0.167	0.208
33	0.13	-	0.333	0.229	0.354	0.208	0.351	0.300	0.125	0.146
34	0.08	-	0.313	0.188	2.292	2.252	0.318	0.282	0.104	0.104
35	0.08	-	0.271	0.146	2.242	2.201	0.270	0.240	0.083	0.083
36	0.08	-	0.292	0.167	1.853	1.824	0.282	0.247	0.083	0.125
37	0.10	-	0.333	0.188	1.901	1.869	0.322	0.278	0.104	0.167
38	0.15	-	0.375	0.229	1.944	1.919	0.360	0.318	0.125	0.208
39	0.17	-	0.417	0.292	1.972	1.935	0.395	0.356	0.146	0.208
40	0.19	-	0.417	0.271	2.158	2.139	0.964	0.938	0.348	0.228
41	0.15	-	0.375	0.250	2.121	2.102	0.931	0.902	0.333	0.199
42	0.15	-	0.333	0.208	2.075	2.054	0.891	0.859	0.315	0.152
43	0.08	-	0.292	0.167	2.02	2.007	0.849	0.825	0.291	0.113
44	0.08	-	1.915	1.910	1.080	1.068	0.315	0.294	0.083	0.125
45	0.13	-	1.960	1.944	1.140	1.125	0.365	0.335	0.125	0.146
46	0.15	-	2.001	1.994	1.195	1.178	0.410	0.388	0.146	0.208
47	0.17	-	2.023	2.015	1.236	1.218	0.452	0.420	0.167	0.208
48	0.60	-	1.767	1.756	1.234	1.22	0.723	0.689	0.327	0.249
49	0.63	-	1.706	1.693	1.174	1.167	0.676	0.657	0.282	0.214
50	0.50	-	1.638	1.627	1.110	1.106	0.626	0.599	0.245	0.170

Table B-3. Discharge readings for tilting flume. Some experiments have no manometer readings because the data was gathered directly from a magnetic flowmeter.

Experiment	Manometer reading (ft)	Discharge (cfs)
1	0.20	0.95
2	0.47	1.46
3	0.92	2.04
4	0.22	1.00
5	0.49	1.49
6	0.49	1.49
7	0.92	2.04
8	0.20	0.95
9	0.48	1.47
10	0.91	2.03
11	0.21	0.97
12	0.49	1.49
13	0.92	2.04
14	0.20	0.95
15	0.48	1.47
16	0.93	2.05
17	0.22	1.00
18	0.49	1.49
19	0.92	2.04
20	0.22	1.00
21	0.50	1.50
22	0.93	2.05

Table B-3 (continued).

Experiment	Manometer reading (ft)	Discharge (cfs)
23	0.18	0.90
24	0.47	1.46
25	0.92	2.04
26	0.16	0.85
27	0.48	1.47
28	0.90	2.02
29	0.17	0.88
30	0.44	1.41
31	0.90	2.02
32		4.93
33		3.91
34		2.88
35		1.88
36		2.00
37		2.95
38		3.92
39		4.84
40		5.04
41		3.98
42		3.01
43		1.92
44		1.82
45		2.92
46		3.96
47		4.95
48		5.08
49		4.03
50		2.91

Table B-4. Replication slope and point gage readings for channel bottom for tilting flume (in feet).

		Measurement number							
Experiment	**Slope**	**3**	**3c**	**4**	**4c**	**5**	**5c**	**6**	**7**
22b	0.021	1.124	1.245	0.663	0.783	0.238	0.359	0.088	0.326
16b	0.015	0.814	0.935	0.487	0.611	0.183	0.305	0.064	0.272
14b	0.015	0.814	0.935	0.487	0.611	0.183	0.305	0.064	0.272
9b	0.009	0.628	0.752	0.426	0.551	0.235	0.358	0.144	0.353

Table B-5. Replication point gage reading for water level for tilting flume (in feet).

	Measurement number									
Experiment	**1**	**2**	**3**	**3c**	**4**	**4c**	**5**	**5c**	**6**	**7**
22b	0.10	0.46	1.483	1.477	1.013	1.007	0.592	0.586	0.663	0.633
16b	0.39	0.49	1.195	1.184	0.863	0.858	0.546	0.534	0.615	0.578
14b	0.25	0.35	1.085	1.083	0.766	0.758	0.450	0.446	0.472	0.444
9b	0.39	0.44	0.977	0.980	0.782	0.777	0.586	0.586	0.621	0.595

Table B-6. Replication discharge readings for tilting flume.

Experiment	Manometer reading (ft)	Discharge (cfs)
22b	0.92	2.038
16b	0.92	2.038
14b	0.21	0.974
9b	0.47	1.457

Table B-7. Point gage readings for channel bottom for all Sloan flume experiments (in feet). Measurements 1, 6, and 7 did not have any point gage readings because the gantry system did not go to those points.

Measurement number						
2	**3**	**3c**	**4**	**4c**	**5**	**5c**
0.031	0.08	0.143	0.08	0.143	0.08	0.143

Table B-8. Point gage readings for water level in Sloan flume (in feet). In cases where the point gage was unable to reach the measurement point, the data is the actual water depth, taken by a ruler.

	Measurement number									
Experiment	**1**	**2**	**3**	**3c**	**4**	**4c**	**5**	**5c**	**6**	**7**
51	0.858	0.945	0.876	0.887	0.833	0.827	0.625	0.613	0.367	0.342
52	0.808	0.947	0.844	0.893	0.827	0.817	0.623	0.613	0.367	0.325
53	0.800	0.944	0.878	0.884	0.824	0.834	0.619	0.618	0.475	0.333
54	0.575	0.936	0.887	0.886	0.818	0.814	0.618	0.612	0.558	0.283
55	0.825	0.914	0.859	0.873	0.792	0.791	0.604	0.599	0.533	0.283
56	0.800	0.917	0.857	0.874	0.798	0.792	0.605	0.601	0.450	0.292
57	0.675	0.917	0.855	0.863	0.801	0.804	0.608	0.599	0.475	0.292
58	0.733	0.799	0.768	0.749	0.702	0.705	0.533	0.523	0.400	0.242
59	0.692	0.802	0.770	0.764	0.700	0.703	0.535	0.523	0.442	0.225
60	0.592	0.735	0.696	0.689	0.648	0.647	0.493	0.486	0.367	0.233
61	0.525	0.737	0.698	0.694	0.647	0.645	0.489	0.487	0.433	0.217
62	0.608	0.659	0.627	0.629	0.580	0.579	0.447	0.445	0.342	0.200
63	0.542	0.658	0.618	0.628	0.575	0.576	0.445	0.437	0.350	0.200
64	0.475	0.653	0.620	0.624	0.583	0.575	0.446	0.442	0.350	0.208
65	0.400	0.458	0.436	0.437	0.408	0.407	0.320	0.315	0.225	0.108
66	0.358	0.453	0.436	0.436	0.410	0.407	0.324	0.316	0.225	0.108
67	1.108	1.119	1.073	1.050	0.977	0.965	0.736	0.729	0.475	0.450
68	0.550	1.092	1.052	1.043	0.966	0.960	0.725	0.716	0.467	0.425

Table B-9. Weigh tank data for Sloan flume.

Experiment	Weight (lb)	Time (s)	Discharge (cfs)
51	3000	20	2.40
52	3000	20	2.40
53	3000	20	2.40
54	3000	20	2.40
55	3000	21	2.29
56	3000	21	2.29
57	3000	21	2.29
58	3000	28	1.72
59	3000	28	1.72
60	3000	33	1.46
61	3000	33	1.46
62	3000	42	1.14
63	3000	42	1.14
64	3000	42	1.14
65	3000	98	0.49
66	3000	99	0.49
67	3000	14	3.43
68	3000	16	3.00

APPENDIX C

DATA CALCULATIONS EXAMPLE

Example calculations using experiment 22 from tilting flume:

Collected data:

$S := 0.021$ Channel slope

$b := 2.95ft$ Channel width

$b_c := 2.815ft$ Average channel width within corrugations

$b_w := 2.685ft$ Channel width at weir

$z := 0.125ft$ Corrugation height

$C_3 := 1.109ft$	$C_{4c} := 0.778ft$	$C_6 := 0.087ft$	Channel readings
$C_{3c} := 1.229ft$	$C_5 := 0.237ft$	$C_7 := 0.326ft$	
$C_4 := 0.656ft$	$C_{5c} := 0.358ft$		

$W_1 := 0.10ft$	$W_{3c} := 1.461ft$	$W_5 := 0.591ft$	Water readings
$W_2 := 0.44ft$	$W_4 := 1.004ft$	$W_{5c} := 0.591ft$	
$W_3 := 1.466ft$	$W_{4c} := 1.004ft$	$W_6 := 0.664ft$	
		$W_7 := 0.636ft$	

$Mano := 0.93ft$ Manometer reading

Calculate average channel reading within corrugations:

$$C_3 := \frac{C_3 + C_{3c}}{2} \qquad \boxed{C_3 = 1.169ft}$$

$$C_4 := \frac{C_4 + C_{4c}}{2} \qquad \boxed{C_4 = 0.717ft}$$

$$C_5 := \frac{C_5 + C_{5c}}{2} \qquad \boxed{C_5 = 0.297ft}$$

Calculate average water reading within corrugations:

$$W_3 := \frac{W_3 + W_{3c}}{2} \qquad W_3 = 1.463\text{ft}$$

$$W_4 := \frac{W_4 + W_{4c}}{2} \qquad W_4 = 1.004\text{ft}$$

$$W_5 := \frac{W_5 + W_{5c}}{2} \qquad W_5 = 0.591\text{ft}$$

Calculate water depth: $y = W - C$

$y_1 := W_1$ $\quad y_4 := W_4 - C_4$ $\quad y_7 := W_7 - C_7$

$y_2 := W_2$ $\quad y_5 := W_5 - C_5$

$y_3 := W_3 - C_3$ $\quad y_6 := W_6 - C_6$

$y_1 = 0.1\text{ft}$ $\quad y_4 = 0.287\text{ft}$ $\quad y_7 = 0.31\text{ft}$

$y_2 = 0.44\text{ft}$ $\quad y_5 = 0.293\text{ft}$

$y_3 = 0.295\text{ft}$ $\quad y_6 = 0.577\text{ft}$

Calculate discharge: $Q = 2.125\sqrt{\text{Mano}}$ derived eq. from Venturi meter

$$Q := 2.125\frac{\text{ft}^{\frac{5}{2}}}{\text{sec}}\cdot\sqrt{\text{Mano}}$$

$$Q = 2.049\frac{\text{ft}^3}{\text{sec}}$$

Calculate cross-sectional area: $A = b\cdot y$

$A_1 := b\cdot y_1$ $\quad A_4 := b_c\cdot y_4$ $\quad A_7 := b_w\cdot y_7$

$A_2 := b\cdot y_2$ $\quad A_5 := b_c\cdot y_5$

$A_3 := b_c\cdot y_3$ $\quad A_6 := b\cdot y_6$

$A_1 = 0.295\text{ft}^2$ $\quad A_4 = 0.808\text{ft}^2$ $\quad A_7 = 0.832\text{ft}^2$

$A_2 = 1.298\text{ft}^2$ $\quad A_5 = 0.826\text{ft}^2$

$A_3 = 0.829\text{ft}^2$ $\quad A_6 = 1.702\text{ft}^2$

Calculate wetted perimeter: $P = b + 2y$

$P_1 := b + 2y_1$ $P_4 := b_c + 2 \cdot y_4$ $P_7 := b_w + 2 \cdot y_7$

$P_2 := b + 2 \cdot y_2$ $P_5 := b_c + 2 \cdot y_5$

$P_3 := b_c + 2 \cdot y_3$ $P_6 := b + 2 \cdot y_6$

$P_1 = 3.15\text{ft}$ $P_4 = 3.389\text{ft}$ $P_7 = 3.305\text{ft}$

$P_2 = 3.83\text{ft}$ $P_5 = 3.402\text{ft}$

$P_3 = 3.404\text{ft}$ $P_6 = 4.104\text{ft}$

Calculate hydraulic radius: $R = \frac{A}{P}$

$R_1 := \frac{A_1}{P_1}$ $R_4 := \frac{A_4}{P_4}$ $R_7 := \frac{A_7}{P_7}$

$R_2 := \frac{A_2}{P_2}$ $R_5 := \frac{A_5}{P_5}$

$R_3 := \frac{A_3}{P_3}$ $R_6 := \frac{A_6}{P_6}$

$R_1 = 0.094\text{ft}$ $R_4 = 0.238\text{ft}$ $R_7 = 0.252\text{ft}$

$R_2 = 0.339\text{ft}$ $R_5 = 0.243\text{ft}$

$R_3 = 0.244\text{ft}$ $R_6 = 0.415\text{ft}$

Calculate velocity: $V = \frac{Q}{A}$

$$V_1 := \frac{Q}{A_1} \quad V_4 := \frac{Q}{A_4} \quad V_7 := \frac{Q}{A_7}$$

$$V_2 := \frac{Q}{A_2} \quad V_5 := \frac{Q}{A_5}$$

$$V_3 := \frac{Q}{A_3} \quad V_6 := \frac{Q}{A_6}$$

$V_1 = 6.947 \frac{ft}{s}$ $V_4 = 2.537 \frac{ft}{s}$ $V_7 = 2.462 \frac{ft}{s}$

$V_2 = 1.579 \frac{ft}{s}$ $V_5 = 2.48 \frac{ft}{s}$

$V_3 = 2.472 \frac{ft}{s}$ $V_6 = 1.204 \frac{ft}{s}$

Calculate Froude number: $Fr = \frac{V}{\sqrt{gy}}$

$$Fr_1 := \frac{V_1}{\sqrt{g \cdot y_1}} \quad Fr_4 := \frac{V_4}{\sqrt{g \cdot y_4}} \quad Fr_7 := \frac{V_7}{\sqrt{g \cdot y_7}}$$

$$Fr_2 := \frac{V_2}{\sqrt{g \cdot y_2}} \quad Fr_5 := \frac{V_5}{\sqrt{g \cdot y_5}}$$

$$Fr_3 := \frac{V_3}{\sqrt{g \cdot y_3}} \quad Fr_6 := \frac{V_6}{\sqrt{g \cdot y_6}}$$

$Fr_1 = 3.873$ $Fr_4 = 0.835$ $Fr_7 = 0.78$

$Fr_2 = 0.42$ $Fr_5 = 0.807$

$Fr_3 = 0.803$ $Fr_6 = 0.279$

Calculate corrugation Manning's 'n': $n = \frac{1.486\frac{ft^{\frac{1}{3}}}{s}\cdot A\cdot R^{\frac{2}{3}}\cdot\sqrt{S}}{Q}$

$$n_3 := \frac{1.486\frac{ft^{\frac{1}{3}}}{s}\cdot A_3\cdot R_3^{\frac{2}{3}}\cdot\sqrt{S}}{Q} \qquad n_4 := \frac{1.486\frac{ft^{\frac{1}{3}}}{s}\cdot A_4\cdot R_4^{\frac{2}{3}}\cdot\sqrt{S}}{Q}$$

$$n_5 := \frac{1.486\frac{ft^{\frac{1}{3}}}{s}\cdot A_5\cdot R_5^{\frac{2}{3}}\cdot\sqrt{S}}{Q}$$

$\boxed{n_3 = 0.034}$ $\boxed{n_4 = 0.033}$ $\boxed{n_5 = 0.034}$

Calculate corrugation average Manning's 'n':

$$n_a := \frac{n_3 + n_4 + n_5}{3} \qquad \boxed{n_a = 0.033}$$

Calculate corrugation submergence ratio: $R_s = \frac{y}{z}$

$$R_{s3} := \frac{y_3}{z} \qquad R_{s4} := \frac{y_4}{z} \qquad R_{s5} := \frac{y_5}{z}$$

$\boxed{R_{s3} = 2.356}$ $\boxed{R_{s4} = 2.296}$ $\boxed{R_{s5} = 2.348}$

Calculate average submergence ratio: $R_{sa} = \frac{\Sigma R_s}{3}$

$$R_{sa} := \frac{R_{s3} + R_{s4} + R_{s5}}{3} \qquad \boxed{R_{sa} = 2.333}$$

Calculate corrugation aspect ratio: $R_A = \frac{b}{y}$

$$R_{A3} := \frac{b_c}{y_3} \qquad R_{A4} := \frac{b_c}{y_4} \qquad R_{A5} := \frac{b_c}{y_5}$$

$$\boxed{R_{A3} = 9.559} \qquad \boxed{R_{A4} = 9.808} \qquad \boxed{R_{A5} = 9.591}$$

Calculate average aspect ratio: $R_{Aa} = \frac{\Sigma R_A}{3}$

$$R_{Aa} := \frac{R_{A3} + R_{A4} + R_{A5}}{3} \qquad \boxed{R_{Aa} = 9.653}$$

Example calculations using experiment 51 from Sloan flume:

Collected data:

$t := 20s$ Weigh tank collection time

$wt := 3000lb$ Weight of water collected

$\rho := 62.4\frac{lb}{ft^3}$ Density of water

$b := 1.48ft$ Channel width

$b_c := 1.355ft$ Average channel width within corrugations

$x_{34} := 6.70ft$

$x_{45} := 9.71ft$ Distance between measured corrugations

$z := 0.0625ft$ Corrugation height

$C_2 := 0.031ft$ $C_4 := 0.080ft$ $C_5 := 0.080ft$

$C_3 := 0.080ft$ $C_{4c} := 0.143ft$ $C_{5c} := 0.143ft$ Channel readings

$C_{3c} := 0.143ft$

$W_1 := 0.858ft$ $W_{3c} := 0.887ft$ $W_5 := 0.625ft$

$W_2 := 0.945ft$ $W_4 := 0.833ft$ $W_{5c} := 0.613ft$ Water readings

$W_3 := 0.876ft$ $W_{4c} := 0.827ft$ $W_6 := 0.367ft$

$W_7 := 0.342ft$

Calculate average channel reading within corrugations:

$$C_3 := \frac{C_3 + C_{3c}}{2} \qquad \boxed{C_3 = 0.111ft}$$

$$C_4 := \frac{C_4 + C_{4c}}{2} \qquad \boxed{C_4 = 0.111ft}$$

$$C_5 := \frac{C_5 + C_{5c}}{2} \qquad \boxed{C_5 = 0.111ft}$$

Calculate average water reading within corrugations:

$$W_3 := \frac{W_3 + W_{3c}}{2} \qquad W_3 = 0.881\text{ft}$$

$$W_4 := \frac{W_4 + W_{4c}}{2} \qquad W_4 = 0.83\text{ft}$$

$$W_5 := \frac{W_5 + W_{5c}}{2} \qquad W_5 = 0.619\text{ft}$$

Calculate water depth: $y = W - C$

$y_1 := W_1$ $\quad y_4 := W_4 - C_4$ $\quad y_7 := W_7$

$y_2 := W_2 - C_2$ $\quad y_5 := W_5 - C_5$

$y_3 := W_3 - C_3$ $\quad y_6 := W_6$

$y_1 = 0.858\text{ft}$ $\quad y_4 = 0.718\text{ft}$ $\quad y_7 = 0.342\text{ft}$

$y_2 = 0.914\text{ft}$ $\quad y_5 = 0.508\text{ft}$

$y_3 = 0.77\text{ft}$ $\quad y_6 = 0.367\text{ft}$

Calculate discharge: $Q = \frac{wt}{t \cdot \rho}$

$$Q := \frac{wt}{t \cdot \rho}$$

$$Q = 2.404 \frac{\text{ft}^3}{\text{sec}}$$

Calculate cross-sectional area: $A = b \cdot y$

$A_1 := b \cdot y_1$ $\quad A_4 := b_c \cdot y_4$ $\quad A_7 := b \cdot y_7$

$A_2 := b \cdot y_2$ $\quad A_5 := b_c \cdot y_5$

$A_3 := b_c \cdot y_3$ $\quad A_6 := b \cdot y_6$

$A_1 = 1.27\text{ft}^2$ $\quad A_4 = 0.974\text{ft}^2$ $\quad A_7 = 0.506\text{ft}^2$

$A_2 = 1.353\text{ft}^2$ $\quad A_5 = 0.688\text{ft}^2$

$A_3 = 1.043\text{ft}^2$ $\quad A_6 = 0.543\text{ft}^2$

Calculate wetted perimeter: $P = b + 2y$

$P_1 := b + 2y_1$ $P_4 := b_c + 2 \cdot y_4$ $P_7 := b + 2 \cdot y_7$

$P_2 := b + 2 \cdot y_2$ $P_5 := b_c + 2 \cdot y_5$

$P_3 := b_c + 2 \cdot y_3$ $P_6 := b + 2 \cdot y_6$

$P_1 = 3.196\text{ft}$ $P_4 = 2.792\text{ft}$ $P_7 = 2.164\text{ft}$

$P_2 = 3.308\text{ft}$ $P_5 = 2.37\text{ft}$

$P_3 = 2.895\text{ft}$ $P_6 = 2.214\text{ft}$

Calculate hydraulic radius: $R = \frac{A}{P}$

$R_1 := \frac{A_1}{P_1}$ $R_4 := \frac{A_4}{P_4}$ $R_7 := \frac{A_7}{P_7}$

$R_2 := \frac{A_2}{P_2}$ $R_5 := \frac{A_5}{P_5}$

$R_3 := \frac{A_3}{P_3}$ $R_6 := \frac{A_6}{P_6}$

$R_1 = 0.397\text{ft}$ $R_4 = 0.349\text{ft}$ $R_7 = 0.234\text{ft}$

$R_2 = 0.409\text{ft}$ $R_5 = 0.29\text{ft}$

$R_3 = 0.36\text{ft}$ $R_6 = 0.245\text{ft}$

Calculate velocity: $V = \frac{Q}{A}$

$V_1 := \frac{Q}{A_1}$ $V_4 := \frac{Q}{A_4}$ $V_7 := \frac{Q}{A_7}$

$V_2 := \frac{Q}{A_2}$ $V_5 := \frac{Q}{A_5}$

$V_3 := \frac{Q}{A_3}$ $V_6 := \frac{Q}{A_6}$

$V_1 = 1.893\frac{\text{ft}}{\text{s}}$ $V_4 = 2.469\frac{\text{ft}}{\text{s}}$ $V_7 = 4.749\frac{\text{ft}}{\text{s}}$

$V_2 = 1.777\frac{\text{ft}}{\text{s}}$ $V_5 = 3.496\frac{\text{ft}}{\text{s}}$

$V_3 = 2.304\frac{\text{ft}}{\text{s}}$ $V_6 = 4.426\frac{\text{ft}}{\text{s}}$

Calculate corrugation average velocity:

$$V_a := \frac{V_3 + V_4 + V_5}{3} \qquad \boxed{V_a = 2.756 \frac{ft}{s}}$$

Calculate Froude number: $Fr = \frac{V}{\sqrt{gy}}$

$$Fr_1 := \frac{V_1}{\sqrt{g \cdot y_1}} \quad Fr_4 := \frac{V_4}{\sqrt{g \cdot y_4}} \quad Fr_7 := \frac{V_7}{\sqrt{g \cdot y_7}}$$

$$Fr_2 := \frac{V_2}{\sqrt{g \cdot y_2}} \quad Fr_5 := \frac{V_5}{\sqrt{g \cdot y_5}}$$

$$Fr_3 := \frac{V_3}{\sqrt{g \cdot y_3}} \quad Fr_6 := \frac{V_6}{\sqrt{g \cdot y_6}}$$

$\boxed{Fr_1 = 0.36}$ $\boxed{Fr_4 = 0.514}$ $\boxed{Fr_7 = 1.432}$

$\boxed{Fr_2 = 0.328}$ $\boxed{Fr_5 = 0.865}$

$\boxed{Fr_3 = 0.463}$ $\boxed{Fr_6 = 1.288}$

Calculate corrugation average velocity:

$$Fr_a := \frac{Fr_3 + Fr_4 + Fr_5}{3} \qquad \boxed{Fr_a = 0.614}$$

Calculate corrugation submergence ratio: $R_s = \frac{y}{z}$

$$R_{s3} := \frac{y_3}{z} \quad R_{s4} := \frac{y_4}{z} \quad R_{s5} := \frac{y_5}{z}$$

$\boxed{R_{s3} = 12.32}$ $\boxed{R_{s4} = 11.496}$ $\boxed{R_{s5} = 8.12}$

Calculate average submergence ratio: $R_{sa} = \frac{\Sigma R_s}{3}$

$$R_{sa} := \frac{R_{s3} + R_{s4} + R_{s5}}{3} \qquad \boxed{R_{sa} = 10.645}$$

Calculate corrugation aspect ratio: $R_A = \frac{b}{y}$

$$R_{A3} := \frac{b_c}{y_3} \qquad R_{A4} := \frac{b_c}{y_4} \qquad R_{A5} := \frac{b_c}{y_5}$$

$R_{A3} = 1.76$ $R_{A4} = 1.886$ $R_{A5} = 2.67$

Calculate corrugation average aspect ratio:

$$R_{Aa} := \frac{R_{A3} + R_{A4} + R_{A5}}{3} \qquad R_{Aa} = 2.105$$

Use Gradually Varied Flow Equation to determine Manning's 'n':

Determine specific energy of each corrugation:

$$E_3 := y_3 + \frac{V_3^2}{2g} \qquad E_3 = 0.852\text{ft}$$

$$E_4 := y_4 + \frac{V_4^2}{2g} \qquad E_4 = 0.813\text{ft}$$

$$E_5 := y_5 + \frac{V_5^2}{2g} \qquad E_5 = 0.697\text{ft}$$

Determine difference in specific energy between corrugations

$$E_{34} := E_4 - E_3 \qquad E_{45} := E_5 - E_4$$

$E_{34} = -0.039\text{ft}$ $E_{45} = -0.116\text{ft}$

Determine energy slope between corrugations:

$$S_{34} := \frac{-E_{34}}{x_{34}} \qquad S_{34} = 5.858 \times 10^{-3}$$

$$S_{45} := \frac{-E_{45}}{x_{45}} \qquad S_{45} = 0.012$$

Determine Manning's 'n' for each section:

$$n_{34} := \frac{1.486\frac{ft}{s}\left(\frac{R_3 + R_4}{2}\right)^{\frac{2}{3}}\sqrt{S_{34}}}{\left(\frac{V_3 + V_4}{2}\right)} \qquad \boxed{n_{34} = 0.024}$$

$$n_{45} := \frac{1.486\frac{ft}{s}\left(\frac{R_4 + R_5}{2}\right)^{\frac{2}{3}}\sqrt{S_{45}}}{\left(\frac{V_4 + V_5}{2}\right)} \qquad \boxed{n_{45} = 0.025}$$

Determine average Manning's 'n':

$$n := \frac{n_{34} + n_{45}}{2} \qquad \boxed{n = 0.025}$$

APPENDIX D

SCALING MANNING'S 'N' DISCUSSION

It is difficult to scale Manning's 'n' due to the fact that it is empirical in nature. In order to maintain a proper scale, similarity between the model and the prototype must be achieved in the geometric, dynamic, and kinematic senses. For simplicity in the model, a single length scale is used, λ_l, where $\lambda_l = \lambda_m / \lambda_p$, l being a characteristic length and the subscripts m and p for model and prototype, respectively.

When considering open channel flow situations, gravity and inertia are major forces acting on the fluid. Surface tension and viscous forces must also be considered. Three dimensionless numbers are considered in this case, Reynolds number (Re), Froude number (Fr), and Weber number (We). When comparing similarity, the ratio of the model to the prototype for these three dimensionless numbers should be equal to unity (Henderson 1966).

In order to have all three ratios equal to unity, the model would have to be run in a different gravitational field or using a fluid with a different density and viscosity of water. These solutions are expensive and impractical, so it is necessary to maintain unity in the dimensionless ratios in order of importance and check to confirm that the model will still be valid even if not all ratios are equal to unity.

Since gravity and inertia forces are dominant in open channel flow, the Froude number ratio should maintain unity:

$$\lambda_{Fr} = \frac{Fr_m}{Fr_p} = 1 \qquad \text{(D-1)}$$

Given the definition of Froude number (Jain 2001):

$$Fr = \frac{V}{\sqrt{gl}} \tag{D-2}$$

Combining (D-1) and (D-2) result in the complete Froude number ratio:

$$\lambda_{Fr} = \frac{V_m}{V_p}\left(\frac{g_p}{g_m}\right)^{\frac{1}{2}}\left(\frac{l_p}{l_m}\right)^{\frac{1}{2}} = \lambda_V \left(\lambda_g\right)^{\frac{-1}{2}}\left(\lambda_l\right)^{\frac{-1}{2}} = 1 \tag{D-3}$$

It is impractical to run tests in a different gravitational field, so $\lambda_g = 1$, which leads to:

$$\lambda_V \left(\lambda_l\right)^{\frac{-1}{2}} = 1 \rightarrow \lambda_V = \left(\lambda_l\right)^{\frac{1}{2}} \tag{D-4}$$

Given (D-4), Manning's 'n' can be scaled as follows (Henderson 1966):

$$\lambda_n = \frac{n_m}{n_p} = \frac{\left(\lambda_l{}^2\right)^{\frac{5}{3}}\left(\lambda_l\right)^{\frac{-2}{3}}}{\lambda_l{}^2 \lambda_V} = \frac{\left(\lambda_l\right)^{\frac{8}{3}}}{\left(\lambda_l\right)^{\frac{5}{2}}} = \left(\lambda_l\right)^{\frac{1}{6}} \tag{D-5}$$

From (D-5), for the half-scale setup in this experiment, Manning's 'n' should be multiplied by 1.12 ($2^{1/6}$) to reach full-scale values.

To check validity of this scaling, the Reynolds number ratio should be checked for unity for viscous effects. Given the definition of Reynolds number (Young, Munson, and Okiishi 2001):

$$\mathrm{Re} = \frac{\rho V l}{\mu} = \frac{V l}{\upsilon} \tag{D-6}$$

From (D-6), the Reynolds model ratio can be written as:

$$\lambda_{\mathrm{Re}} = \lambda_V \lambda_l \left(\lambda_\nu\right)^{-1} = 1 \tag{D-7}$$

Most models in open channel flow use identical fluids to their prototype counterpart, so $\lambda_\nu = 1$, so (D-7) can be written as:

$$\lambda_V \lambda_l = 1 \rightarrow \lambda_V = \lambda_l{}^{-1} \tag{D-8}$$

(D-4) and (D-8) create a problem in that the velocity ratio is not equal. Because of this, the Reynolds number ratio must not be held to unity:

$$\lambda_{\mathrm{Re}} = \lambda_V \lambda_l (\lambda_\nu)^{-1} = (\lambda_l)^{\frac{1}{2}} \lambda_l = (\lambda_l)^{\frac{3}{2}} \qquad \text{(D-9)}$$

(D-9) may create problems when scaling model results to a prototype. In order to determine if Manning's 'n' will be affected from this difference, the relationship between Reynolds number and Manning's 'n' must be observed. Manning's 'n' is related to the Darcy-Weisbach friction factor *f* as the following equation:

$$f = \frac{8gn^2}{R^{\frac{1}{3}}} \qquad \text{(D-10)}$$

Reynolds number is related to *f* and the relative roughness ($\varepsilon / 4R$) with the Moody diagram. Since the relative roughness is dimensionless and geometrical, the relative roughness ratio is equal to unity. Observing the Moody diagram, friction factor *f* becomes independent of Reynolds number in the region of wholly turbulent flow. Since *f* is independent of Reynolds number in this region and since the relative roughness ratio is equal to unity, Manning's 'n' will be independent of Reynolds number in the wholly turbulent flow region. Therefore, if the model and the prototype act under wholly turbulent flow, Reynolds number will not have an effect on the scaling of Manning's 'n' (Henderson 1966).

The Weber number should also be checked for unity for surface tension effects. Given the definition of Weber number (Young, Munson, and Okiishi 2001):

$$We = \frac{\rho V^2 l}{\sigma} \qquad \text{(D-11)}$$

From (D-11), the Weber model ratio can be written as:

$$\lambda_{We} = \lambda_\rho (\lambda_V)^2 \lambda_l (\lambda_\sigma)^{-1} = 1 \qquad \text{(D-12)}$$

As mentioned above, models and prototypes usually share the same type of fluid, which leads to λ_ρ and λ_σ equal to unity. Thus, (D-12) can be rewritten as:

$$\lambda_{We} = (\lambda_V)^2 \lambda_l = 1 \rightarrow \lambda_V = (\lambda_l)^{\frac{-1}{2}} \qquad \text{(D-13)}$$

As in the case of the Reynolds number, the Weber number creates a different relationship of the velocity ratio to the length ratio than does the Froude number. As with the Reynolds number, the Weber number ratio cannot be unity:

$$\lambda_{We} = \lambda_\rho (\lambda_V)^2 \lambda_l (\lambda_\sigma)^{-1} = \lambda_l \lambda_l = \lambda_l{}^2 \qquad \text{(D-14)}$$

In his text, Henderson mentions that surface tension can be ignored if model water depths are maintained above 0.167 feet. If the water level is kept above 0.167 feet, the Weber number has no effect on Manning's 'n' (1966).

Notations

The following symbols are used in this appendix:

λ_l = length scale

$(X)_m$ = characteristic of model (Fr, e.g.)

$(X)_p$ = characteristic of prototype

λ_{Fr} = Froude number ratio

Fr = Froude number

V = velocity (ft/s)

g = gravitational constant (ft/s^2)

l = characteristic length (ft)

λ_V = velocity scale

λ_g = gravitational constant scale

λ_n = Manning's 'n' scale

Re = Reynolds number

ρ = density (slugs/ft^3)

μ = dynamic viscosity (lb s/ft^2)

v = kinematic viscosity (ft^2/s)

λ_{Re} = Reynolds number ratio

λ_v = kinematic viscosity scale

f = Darcy-Weisbach friction factor

R = hydraulic radius (ft)

ε = roughness (ft)

We = Weber number

σ = surface tension (lb/ft)

λ_{We} = Weber number ratio

λ_ρ = density scale

λ_σ = surface tension scale

References

Henderson, F. M. (1966). *Open Channel Flow,* Macmillan Company, New York.

Jain, S. C. (2001). *Open-Channel Flow,* Wiley, New York.

Young, D. F., B. R. Munson, and T. H. Okiishi (2001). *A Brief Introduction to Fluid Mechanics*, Wiley, New York.

APPENDIX E

DESIGN EXAMPLE

Given: Concrete box culvert, 6' wide, 3" corrugations on the bottom and both sides
Q=25 cfs, S=0.5%

Determine: Manning's 'n'

Solution: Defining knowns: $b := 6ft$ $z := .25ft$ $Q := 25\frac{ft^3}{sec}$ $S := 0.005$

$y := 1ft$ initial guess

$R_A := \frac{b}{y}$ definition of aspect ratio

$R_S := \frac{y}{z}$ definition of submergence ratio

$A := b \cdot y$ definition of area

$P := b + 2y$ definition of perimeter

$R := \frac{A}{P}$ definition of hydraulic radius

$$Q = \frac{1.486}{n} A R^{\frac{2}{3}} \sqrt{S}$$ Manning equation (equation 3)

$$n = \frac{1.486 A \cdot R^{\frac{2}{3}} \cdot \sqrt{S}}{Q}$$ Solving for n

$$n = \frac{1.486 (6 \cdot y) \cdot \left(\frac{6 \cdot y}{6 + 2 \cdot y} \right)^{\frac{2}{3}} \cdot \sqrt{0.005}}{25}$$

$$\boxed{n = 0.08327 y^{\frac{5}{3}} \cdot (6 + 2y)^{\frac{-2}{3}}}$$ Solving for n in terms of y

Using equation 5:

$$n = 0.029\left(\frac{R_S}{R_A}\right)^{-0.184}$$

$$0.08327y^{\frac{5}{3}}\cdot(6+2y)^{\frac{-2}{3}} = 0.029\left[\frac{y^2}{(6\cdot 0.25)}\right]^{-0.184}$$ Putting in terms of y

Solving for y:

$y := 1.24ft$

Solving for n:

$$n = 0.029\left[\frac{(1.24)^2}{6\cdot(0.25)}\right]^{-0.184}$$

$n := 0.028$

APPENDIX F

ERROR ANALYSIS FOR MANNING'S 'N'

Table F-1. Uncertainties in collected data.

Measurement (units)	Uncertainty
Slope distance, S_{Sx} (ft)	0.05
Rod height, S_{Sy} (ft)	0.01
Channel width, S_b (ft)	0.01
Water depth, S_y (ft)	0.01
Manometer reading, S_{mano} (ft)	0.01
Flowmeter reading, S_Q (cfs)	0.10
Weigh tank weight, S_{wt} (lb)	5
Weigh tank time, S_t (s)	0.5

In order to determine the error of Manning's 'n', the Manning equation must be solved for 'n':

$$n = \frac{1.486 A R^{\frac{2}{3}} \sqrt{S}}{Q} \qquad \text{(F-1)}$$

(F-1) can be rewritten as:

$$n = 1.486 A^{\frac{5}{3}} P^{\frac{-2}{3}} S^{\frac{1}{2}} Q^{-1} \qquad \text{(F-2)}$$

From (F-2), Manning's 'n' is a function of A, P, S, and Q. Therefore, the uncertainty of Manning's 'n' can be described as:

$$S_n = [(\frac{\partial n}{\partial A} S_A)^2 + (\frac{\partial n}{\partial P} S_P)^2 + (\frac{\partial n}{\partial S} S_S)^2 + (\frac{\partial n}{\partial Q} S_Q)^2]^{\frac{1}{2}} \qquad \text{(F-3)}$$

The first term on the right hand side of (F-3) can be manipulated to:

$$\frac{\partial n}{\partial A} S_A = \frac{\partial [1.486 A^{\frac{5}{3}} P^{\frac{-2}{3}} S^{\frac{1}{2}} Q^{-1}]}{\partial A} S_A = \frac{5}{3} (1.486 A^{\frac{2}{3}} P^{\frac{-2}{3}} S^{\frac{1}{2}} Q^{-1}) \frac{A}{A} = \frac{5n}{3A} S_A$$

The second term on the right hand side of (F-3) can be manipulated to:

$$\frac{\partial n}{\partial P}S_P = \frac{\partial[1.486A^{\frac{5}{3}}P^{\frac{-2}{3}}S^{\frac{1}{2}}Q^{-1}]}{\partial P}S_P = \frac{-2}{3}(1.486A^{\frac{5}{3}}P^{\frac{-5}{3}}S^{\frac{1}{2}}Q^{-1})\frac{P}{P} = \frac{-2n}{3P}S_P$$

The third term on the right hand side of (F-3) can be manipulated to:

$$\frac{\partial n}{\partial S}S_S = \frac{\partial[1.486A^{\frac{5}{3}}P^{\frac{-2}{3}}S^{\frac{1}{2}}Q^{-1}]}{\partial S}S_S = \frac{1}{2}(1.486A^{\frac{5}{3}}P^{\frac{-2}{3}}S^{\frac{-1}{2}}Q^{-1})\frac{S}{S} = \frac{n}{2S}S_S$$

The fourth term on the right hand side of (F-3) can be manipulated to:

$$\frac{\partial n}{\partial Q}S_Q = \frac{\partial[1.486A^{\frac{5}{3}}P^{\frac{-2}{3}}S^{\frac{1}{2}}Q^{-1}]}{\partial Q}S_Q = -(1.486A^{\frac{5}{3}}P^{\frac{-2}{3}}S^{\frac{-1}{2}}Q^{-2})\frac{Q}{Q} = \frac{-n}{Q}S_Q$$

From this, (F-3) becomes:

$$S_n = [(\frac{5n}{3A}S_A)^2 + (\frac{-2n}{3P}S_P)^2 + (\frac{n}{2S}S_S)^2 + (\frac{-n}{Q}S_Q)^2]^{\frac{1}{2}} \qquad \text{(F-4)}$$

(F-4) can be rewritten as:

$$\frac{S_n}{n} = [(\frac{5S_A}{3A})^2 + (\frac{-2S_P}{3P})^2 + (\frac{S_S}{2S})^2 + (\frac{-S_Q}{Q})^2]^{\frac{1}{2}} \qquad \text{(F-5)}$$

Each of these terms (A, P, S, and Q) require their own measurements, so a separate error analysis for each term is required. Given the equation for area, A = by, the uncertainty of area can be described by the following equation:

$$S_A = [(\frac{\partial A}{\partial b}S_b)^2 + (\frac{\partial A}{\partial y}S_y)^2]^{\frac{1}{2}} \qquad \text{(F-6)}$$

Following similar steps as above, (F-6) can be rewritten as:

$$\frac{S_A}{A} = [(\frac{S_b}{b})^2 + (\frac{S_y}{y})^2]^{\frac{1}{2}} \qquad \text{(F-7)}$$

Given the equation for perimeter, P = b + 2y, the uncertainty of perimeter can be described as:

$$S_P = [(\frac{\partial P}{\partial b} S_b)^2 + (\frac{\partial P}{\partial y} S_y)^2 + (\frac{\partial P}{\partial y} S_y)^2]^{\frac{1}{2}} \quad \text{(F-8)}$$

(F-8) can be rewritten as:

$$S_P = [S_b{}^2 + 2S_y{}^2]^{\frac{1}{2}} \quad \text{(F-9)}$$

Given the equation for slope, S = Sy / Sx, the uncertainty of slope can be described as:

$$S_S = [(\frac{\partial S}{\partial Sy} S_{Sy})^2 + (\frac{\partial S}{\partial Sx} S_{Sx})^2]^{\frac{1}{2}} \quad \text{(F-10)}$$

(F-10) can be rewritten as:

$$\frac{S_S}{S} = [(\frac{S_{Sy}}{Sy})^2 + (\frac{-S_{Sx}}{Sx})^2]^{\frac{1}{2}} \quad \text{(F-11)}$$

Discharge was gathered in three different ways depending on the flume and on the pump used. Some discharge data were collected using a manometer connected to a Venturi meter, some were collected from a weigh tank, and some were collected directly from a flow meter. Discharges collected directly from a flow meter do not require an additional error analysis, but discharges collected from a weigh tank or from a Venturi meter require additional error analysis.

If the discharge was collected from a Venturi meter, the following equation was used:

$$Q = 2.125(Mano)^{\frac{1}{2}} \quad \text{(F-12a)}$$

Assuming there is no error in the coefficient, the error analysis for discharge determined by the Venturi meter used is:

$$S_Q = [(\frac{\partial Q}{\partial Mano} S_{Mano})^2]^{\frac{1}{2}} \quad \text{(F-13a)}$$

(F-13a) can be rewritten as:

$$\frac{S_Q}{Q} = [(\frac{S_{Mano}}{2Mano})^2]^{\frac{1}{2}} = \frac{S_{Mano}}{2Mano} \qquad \text{(F-14a)}$$

If the discharge was collected from a weigh tank, the following equation was used:

$$Q = \frac{wt}{62.4t} \qquad \text{(F-12b)}$$

The error analysis for discharge determined by a weigh tank is:

$$S_Q = [(\frac{\partial Q}{\partial wt} S_{wt})^2 + (\frac{\partial Q}{\partial t} S_t)^2]^{\frac{1}{2}} \qquad \text{(F-13b)}$$

(F-13b) can be rewritten as:

$$\frac{S_Q}{Q} = [(\frac{S_{wt}}{wt})^2 + (\frac{-S_t}{t})^2]^{\frac{1}{2}} \qquad \text{(F-14b)}$$

Combining (F-5) with (F-7), (F-9), (F-11), and (F-14) gives the following relationships:

For discharge from the Venturi meter:

$$\frac{S_n}{n} = [(\frac{5}{3}[(\frac{S_b}{b})^2 + (\frac{S_y}{y})^2]^{\frac{1}{2}})^2 + (\frac{-2[S_b{}^2 + 2S_y{}^2]^{\frac{1}{2}}}{3P})^2 + (\frac{1}{2}[(\frac{S_{Sy}}{Sy})^2 + (\frac{-S_{Sx}}{Sx})^2]^{\frac{1}{2}})^2 + (\frac{-S_{Mano}}{2Mano})^2]^{\frac{1}{2}} \qquad \text{(F-15a)}$$

For discharge from the weigh tank:

$$\frac{S_n}{n} = [(\frac{5}{3}[(\frac{S_b}{b})^2 + (\frac{S_y}{y})^2]^{\frac{1}{2}})^2 + (\frac{-2[S_b{}^2 + 2S_y{}^2]^{\frac{1}{2}}}{3P})^2 + (\frac{1}{2}[(\frac{S_{Sy}}{Sy})^2 + (\frac{-S_{Sx}}{Sx})^2]^{\frac{1}{2}})^2 + (-[(\frac{S_{wt}}{wt})^2 + (\frac{-S_t}{t})^2]^{\frac{1}{2}})^2]^{\frac{1}{2}} \qquad \text{(F-15b)}$$

For discharge from the flow meter:

$$\frac{S_n}{n} = [(\frac{5}{3}[(\frac{S_b}{b})^2 + (\frac{S_y}{y})^2]^{\frac{1}{2}})^2 + (\frac{-2[S_b{}^2 + 2S_y{}^2]^{\frac{1}{2}}}{3P})^2 + (\frac{1}{2}[(\frac{S_{Sy}}{Sy})^2 + (\frac{-S_{Sx}}{Sx})^2]^{\frac{1}{2}})^2 + (\frac{-S_Q}{Q})^2]^{\frac{1}{2}} \quad \text{(F-15c)}$$

Error anaylsis calculation example using experiment 22:

Using Venturi meter, so use equation F-15a.

$S_b := 0.01ft$ $S_{Sx} := 0.05ft$

$S_y := 0.01ft$ $S_{Mano} := 0.01ft$ Uncertainties in measurements

$S_{Sy} := 0.01ft$

$b := 2.815ft$ Channel widths

$y_3 := 0.297ft$

$y_4 := 0.285ft$ Water depths

$y_5 := 0.293ft$

$P_3 := b + 2y_3$ $P_4 := b + 2y_4$ $P_5 := b + 2y_5$

$P_3 = 3.409ft$ $P_4 = 3.385ft$ $P_5 = 3.401ft$ Perimeter data

$Sx := 40ft$ $S := 0.021$

$Sy := S \cdot Sx$ $Sy = 0.84ft$ Slope data

$Mano := 0.93ft$ Manometer reading

$n_3 := 0.034$ $n_4 := 0.033$ $n_5 := 0.034$ Manning 'n' values

Determine uncertainty:

$$S_{n3} := \left[\left[\frac{5}{3} \cdot \left[\left[\left(\frac{S_b}{b} \right)^2 + \left(\frac{S_y}{y_3} \right)^2 \right]^{\frac{1}{2}} \right] \right]^2 + \left[\frac{-2 \cdot \left(S_b{}^2 + 2 \cdot S_y{}^2 \right)^{\frac{1}{2}}}{3 \cdot P_3} \right]^2 \dots \right]^{\frac{1}{2}} \cdot n_3$$
$$+ \left[\left[\frac{1}{2} \cdot \left[\left(\frac{S_{Sy}}{Sy} \right)^2 + \left(\frac{-S_{Sx}}{Sx} \right)^2 \right]^{\frac{1}{2}} \right]^2 + \left(\frac{-S_{Mano}}{2Mano} \right)^2 \right]$$

$$S_{n4} := \left[\left[\frac{5}{3} \cdot \left[\left[\left(\frac{S_b}{b} \right)^2 + \left(\frac{S_y}{y_4} \right)^2 \right]^{\frac{1}{2}} \right] \right]^2 + \left[\frac{-2 \cdot \left(S_b{}^2 + 2 \cdot S_y{}^2 \right)^{\frac{1}{2}}}{3 \cdot P_4} \right]^2 \dots \right]^{\frac{1}{2}} \cdot n_4$$
$$+ \left[\left[\frac{1}{2} \cdot \left[\left(\frac{S_{Sy}}{Sy} \right)^2 + \left(\frac{-S_{Sx}}{Sx} \right)^2 \right]^{\frac{1}{2}} \right]^2 + \left(\frac{-S_{Mano}}{2Mano} \right)^2 \right]$$

$$S_{n5} := \left[\left[\frac{5}{3} \cdot \left[\left[\left(\frac{S_b}{b} \right)^2 + \left(\frac{S_y}{y_5} \right)^2 \right]^{\frac{1}{2}} \right] \right]^2 + \left[\frac{-2 \cdot \left(S_b{}^2 + 2 \cdot S_y{}^2 \right)^{\frac{1}{2}}}{3 \cdot P_5} \right]^2 \dots \right]^{\frac{1}{2}} \cdot n_5$$
$$+ \left[\left[\frac{1}{2} \cdot \left[\left(\frac{S_{Sy}}{Sy} \right)^2 + \left(\frac{-S_{Sx}}{Sx} \right)^2 \right]^{\frac{1}{2}} \right]^2 + \left(\frac{-S_{Mano}}{2Mano} \right)^2 \right]$$

$S_{n3} = 1.941 \times 10^{-3}$ $S_{n4} = 1.961 \times 10^{-3}$ $S_{n5} = 1.967 \times 10^{-3}$

After the error for each point is found, the error for the average Manning's 'n' can be found. The error for Manning's 'n' can be described as:

$$S_{na} = [\frac{1}{3}(\frac{\partial n_a}{\partial n_3} S_{n3})^2 + \frac{1}{3}(\frac{\partial n_a}{\partial n_4} S_{n4})^2 + \frac{1}{3}(\frac{\partial n_a}{\partial n_5} S_{n5})^2]^{\frac{1}{2}} \qquad \text{(F-16)}$$

(F-16) can be rewritten as:

$$S_{na} = (\frac{S_{n3}^2 + S_{n4}^2 + S_{n5}^2}{3})^{\frac{1}{2}} \qquad \text{(F-17)}$$

Table F-2. Calculated error for Manning's 'n' for tilting flume experiments.

	Sn (multiplied by 1000)				*Sn/n*			
Experiment	**3**	**4**	**5**	**Average**	**3**	**4**	**5**	**Average**
1	2.26	2.19	2.17	2.21	7.3%	7.4%	7.4%	7.4%
2	1.69	1.66	1.62	1.66	6.3%	6.4%	6.4%	6.4%
3	1.47	1.47	1.48	1.47	5.8%	5.8%	5.8%	5.8%
4	2.20	2.21	2.17	2.19	7.1%	7.1%	7.2%	7.2%
5	1.68	1.69	1.78	1.72	5.6%	5.5%	5.2%	5.4%
6	1.67	1.68	1.62	1.66	5.6%	5.6%	5.8%	5.7%
7	1.36	1.38	1.41	1.38	4.8%	4.7%	4.6%	4.7%
8	2.59	2.64	2.63	2.62	7.7%	7.5%	7.5%	7.6%
9	1.84	1.88	1.86	1.86	6.0%	5.8%	5.9%	5.9%
10	1.50	1.49	1.47	1.49	4.9%	5.0%	5.1%	5.0%
11	2.83	2.75	2.72	2.77	7.7%	8.0%	8.1%	7.9%
12	2.00	1.99	1.98	1.99	6.2%	6.2%	6.3%	6.2%
13	1.58	1.59	1.55	1.57	5.3%	5.3%	5.5%	5.4%
14	3.06	3.06	2.95	3.03	8.4%	8.4%	8.8%	8.5%
15	2.21	2.18	2.15	2.18	6.4%	6.5%	6.7%	6.5%
16	1.75	1.73	1.68	1.72	5.3%	5.4%	5.7%	5.5%
17	3.22	3.18	3.27	3.22	8.2%	8.3%	8.1%	8.2%
18	2.34	2.31	2.25	2.30	6.7%	6.8%	7.1%	6.8%
19	1.87	1.85	1.92	1.88	5.6%	5.7%	5.4%	5.5%
20	3.34	3.30	3.35	3.33	8.6%	8.7%	8.5%	8.6%
21	2.45	2.41	2.47	2.44	6.8%	6.9%	6.7%	6.8%
22	1.96	1.93	1.95	1.94	5.8%	5.9%	5.8%	5.8%
23	4.25	4.18	4.10	4.17	9.3%	9.6%	9.8%	9.6%
24	2.86	2.84	2.75	2.82	7.4%	7.4%	7.9%	7.6%
25	2.27	2.21	2.13	2.20	6.1%	6.3%	6.8%	6.4%
26	5.31	4.94	4.85	5.04	9.3%	10.2%	10.5%	10.0%
27	3.13	3.12	3.03	3.10	7.9%	7.9%	8.3%	8.0%
28	2.51	2.47	2.42	2.47	6.6%	6.8%	7.0%	6.8%
29	5.40	5.59	5.10	5.37	9.5%	9.1%	10.3%	9.6%
30	3.67	3.66	3.39	3.58	7.4%	7.4%	8.4%	7.7%
31	2.64	2.78	2.57	2.66	6.9%	6.3%	7.2%	6.8%
32	1.86	1.91	1.90	1.89	6.1%	5.9%	6.0%	6.0%

Table F-2 (continued).

	Sn (multiplied by 1000)				*Sn/n*			
Experiment	**3**	**4**	**5**	**Average**	**3**	**4**	**5**	**Average**
33	2.36	2.36	2.29	2.33	6.5%	6.5%	6.7%	6.6%
34	3.10	3.10	3.04	3.08	7.5%	7.5%	7.7%	7.6%
35	4.54	4.37	4.36	4.43	9.6%	9.9%	9.9%	9.8%
36	4.07	3.86	3.77	3.90	8.9%	9.2%	9.4%	9.1%
37	2.77	2.79	2.65	2.73	7.3%	7.2%	7.6%	7.4%
38	2.21	2.24	2.11	2.19	6.1%	6.0%	6.4%	6.2%
39	1.94	1.85	1.81	1.86	5.2%	5.5%	5.6%	5.4%
40	1.57	1.64	1.58	1.60	5.3%	5.0%	5.3%	5.2%
41	1.92	2.01	1.92	1.95	5.9%	5.7%	5.9%	5.8%
42	2.41	2.51	2.41	2.44	7.0%	6.8%	7.0%	6.9%
43	3.72	3.77	3.77	3.75	9.0%	8.9%	8.9%	8.9%
44	3.55	3.47	3.39	3.47	8.6%	8.7%	8.8%	8.7%
45	2.15	2.23	2.12	2.17	6.7%	6.5%	6.8%	6.6%
46	1.66	1.74	1.65	1.68	5.6%	5.3%	5.6%	5.5%
47	1.33	1.44	1.37	1.38	5.1%	4.7%	5.0%	4.9%
48	1.25	1.20	1.09	1.18	4.1%	4.2%	4.7%	4.3%
49	1.50	1.44	1.34	1.43	4.8%	4.9%	5.3%	5.0%
50	1.98	1.90	1.76	1.88	5.9%	6.1%	6.4%	6.1%

APPENDIX G

DETERMINATION OF "BARRIER" FROUDE NUMBER

Given: Concrete box culvert, 6' wide, 3" corrugations on the bottom and both sides

Determine: "Barrier" Froude number where hydraulic jump will not occur when reaching corrugation.

Solution: Defining known: $b_1 := 6\,ft$ $b_c := 5.5\,ft$ $Fr_c := 1$ $delz := .25\,ft$

$E_1 := E_c + delz$ (Jain, p. 90)

$E_c := y_c + \frac{V_c^2}{2g}$ (Jain, p. 90)

$E_c := y_c + \frac{Q^2}{A_c^2 \cdot 2g}$ (Continuity equation, V=Q/A)

$Fr := \frac{V}{\sqrt{g \cdot y}}$ (Jain, p. 84)

Fr = 1 --> $V_c := \sqrt{g \cdot y_c}$

$Q := A_c \cdot \sqrt{g \cdot y_c}$

Solve for yc

$$y_c := 0.1009\ Q^{\frac{2}{3}}$$

$$E_c := 0.1009\ Q^{\frac{2}{3}} + \frac{Q^2}{\left[b_c \cdot \left(.1009\ Q^{\frac{2}{3}}\right)\right]^2 \cdot 2g}$$

Replacing yc in specific energy equation

$$E_c := 0.1009\ Q^{\frac{2}{3}} + 0.0424\ Q^{\frac{2}{3}}$$

$$E_c := 0.1433\ Q^{\frac{2}{3}}$$

$$E_1 := 0.1433\ Q^{\frac{2}{3}} + 0.25$$

$$y_1 + \frac{Q^2}{\left(b_1 \cdot y_1\right)^2 \cdot 2g} = 0.1433\ Q^{\frac{2}{3}} + 0.25$$

Create a root equation

$$y_1^3 + 4.313 \cdot 10^{-4} Q^2 - 0.1433\ Q^{\frac{2}{3}}\ y_1^2 - 0.25\ y_1^2 = 0$$

Solve for y1, determine "barrier" Froude number

Table G-1. Numerical values of equations for various discharges.

Disch. Q (cfs)	*Crit. depth y_c (ft)*	*Crit. spec. ener. E_c (ft)*	*Upstr. spec. ener. E_1 (ft)*	*Upstr. depth y_1 (ft)*	*Froude num. Fr_B*
chosen	**$Q^{2/3}/(b_c^{2/3}g^{1/3})$**	**$y_c + V_c^2/2g$**	**$E_c + z$**	**Solved**	**$Q/(b_1y_1^{3/2}g^{1/2})$**
5	0.295	0.442	0.692	0.140	***2.814***
10	0.468	0.702	0.952	0.247	***2.388***
15	0.614	0.920	1.170	0.342	***2.199***
20	0.743	1.115	1.365	0.429	***2.087***
25	0.863	1.294	1.544	0.511	***2.011***
30	0.974	1.461	1.711	0.588	***1.955***
35	1.079	1.619	1.869	0.661	***1.911***
40	1.180	1.770	2.020	0.732	***1.876***
45	1.276	1.914	2.164	0.800	***1.847***
50	1.369	2.054	2.304	0.866	***1.822***
55	1.459	2.188	2.438	0.930	***1.801***
60	1.546	2.319	2.569	0.992	***1.783***
65	1.631	2.446	2.696	1.053	***1.767***
70	1.713	2.570	2.820	1.113	***1.752***
75	1.794	2.691	2.941	1.171	***1.739***
80	1.873	2.809	3.059	1.228	***1.728***
85	1.950	2.925	3.175	1.283	***1.717***
90	2.026	3.039	3.289	1.338	***1.707***
95	2.100	3.151	3.401	1.392	***1.698***
100	2.173	3.260	3.510	1.445	***1.690***

APPENDIX H

BCAP PROGRAM OUTPUTS

Experiment 22, test (a) setup:

NEBRASKA DEPARTMENT OF ROADS
Broken-Back Culvert Analysis Program (BCAP)
PROJECT INFO
Project: Increasing Rougness
Station or Location: Experiment 22a
Date: 05 / 04 / 2006
DISCHARGE DATA
Minimum: 0.000 cms
Design Discharge: 0.328 cms
Maximum: 1.000 cms
Number of Barrels: 1
TAILWATER DATA
Type: Downstream
Channel Shape: Rectangle
Bottom Width: 1.80 m
Bottom Slope: 0.021 m/m
Roughness Coefficient: 0.012
CULVERT DATA
Type: Concrete Box
Span (per barrel): 1.80 m
Rise: 1.80 m
Inlet Type: Headwall, Square Edge (90-45 deg.)
Roughness Coefficient: 0.012
Outlet Section Roughness Coeff.: 0.0376
Inlet Section Slope: N.A.
Steep Section Slope: 0 m/m
Outlet Section Slope: 0 m/m
CULVERT PROFILE DATA
Type: Single Broken-Back
Inlet Station: 0.000 m
Inlet Elevation: 10.000 m
Lower Break Station: 10.000 m
Lower Break Elevation: 9.790 m
Outlet Station: 37.200 m
Outlet Elevation: 9.220 m

Experiment 22, test (a) results:

NEBRASKA DEPARTMENT OF ROADS
Broken-Back Culvert Analysis Program (BCAP)
PROJECT INFO
Project: Increasing Rougness
Station or Location: Experiment 22a
Date: 05/04/2006
CULVERT DATA
Discharge: .328 cms
Shape: Box
Material: Concrete
Size: 1-1.8 m x 1.8 m
Inlet Type: Headwall, Square Edge (90-45 deg.)
WATER SURFACE PROFILE
Inlet Depth: 0.15 m
Inlet Velocity: 1.21 m/s
Upper Break Depth: 0.15 m
Upper Break Velocity: 1.21 m/s
Lower Break Depth: 0.17 m
Lower Break Velocity: 1.06 m/s
Depth at End of Hydraulic Jump: N/A m
Velocity at End of Hydraulic Jump: N/A m/s
Depth at End of Hydraulic Jump: 0.08 m
Velocity at End of Hydraulic Jump: 2.22 m/s
OUTPUT DATA
Head Water Depth: 0.25 m
Inlet Control Elevation: 10.25 m
Break Control Elevation: 0 m
Critical Depth: 0.15 m
Tailwater Depth: 0.08 m
Hydraulic Jump? NO
Outlet Depth: 0.17 m
Outlet Velocity: 1.04 m/s
Outlet Froude No.: .8

Experiment 22, test (b) setup:

NEBRASKA DEPARTMENT OF ROADS
Broken-Back Culvert Analysis Program (BCAP)
PROJECT INFO
Project: Increasing Rougness
Station or Location: Experiment 22b
Date: 05 / 04 / 2006
DISCHARGE DATA
Minimum: 0.000 cms
Design Discharge: 0.328 cms
Maximum: 1.000 cms
Number of Barrels: 1
TAILWATER DATA
Type: Downstream
Channel Shape: Rectangle
Bottom Width: 1.80 m
Bottom Slope: 0.021 m/m
Roughness Coefficient: 0.012
CULVERT DATA
Type: Concrete Box
Span (per barrel): 1.80 m
Rise: 1.80 m
Inlet Type: Headwall, Square Edge (90-45 deg.)
Roughness Coefficient: 0.012
Outlet Section Roughness Coeff.: 0.0376
Inlet Section Slope: N.A.
Steep Section Slope: 0.571 m/m
Outlet Section Slope: 0.021 m/m
CULVERT PROFILE DATA
Type: Single Broken-Back
Inlet Station: 0.000 m
Inlet Elevation: 15.500 m
Lower Break Station: 10.000 m
Lower Break Elevation: 9.790 m
Outlet Station: 37.200 m
Outlet Elevation: 9.220 m

Experiment 22, test (b) results:

NEBRASKA DEPARTMENT OF ROADS
Broken-Back Culvert Analysis Program (BCAP)
PROJECT INFO
Project: Increasing Rougness
Station or Location: Experiment 22b
Date: 05/04/2006
CULVERT DATA
Discharge: .328 cms
Shape: Box
Material: Concrete
Size: 1-1.8 m x 1.8 m
Inlet Type: Headwall, Square Edge (90-45 deg.)
WATER SURFACE PROFILE
Inlet Depth: 0.15 m
Inlet Velocity: 1.21 m/s
Upper Break Depth: 0.15 m
Upper Break Velocity: 1.21 m/s
Lower Break Depth: 0.06 m
Lower Break Velocity: 3.10 m/s
Depth at End of Hydraulic Jump: 0.73 m
Velocity at End of Hydraulic Jump: .90 m/s
Depth at End of Hydraulic Jump: 0.08 m
Velocity at End of Hydraulic Jump: 2.22 m/s
OUTPUT DATA
Head Water Depth: 0.16 m
Inlet Control Elevation: 15.66 m
Break Control Elevation: 0 m
Critical Depth: 0.15 m
Tailwater Depth: 0.08 m
Hydraulic Jump? YES
Jump Station: 11.24 m
Jump Length: 0.70 m
Outlet Depth: 0.15 m
Outlet Velocity: 1.21 m/s
Outlet Froude No.: 1.0

Experiment 27, test (a) setup:

NEBRASKA DEPARTMENT OF ROADS
Broken-Back Culvert Analysis Program (BCAP)
PROJECT INFO
Project: Increasing Rougness
Station or Location: Experiment 27a
Date: 05 / 04 / 2006
DISCHARGE DATA
Minimum: 0.000 cms
Design Discharge: 0.236 cms
Maximum: 1.000 cms
Number of Barrels: 1
TAILWATER DATA
Type: Downstream
Channel Shape: Rectangle
Bottom Width: 1.80 m
Bottom Slope: 0.04 m/m
Roughness Coefficient: 0.012
CULVERT DATA
Type: Concrete Box
Span (per barrel): 1.80 m
Rise: 1.80 m
Inlet Type: Headwall, Square Edge (90-45 deg.)
Roughness Coefficient: 0.012
Outlet Section Roughness Coeff.: 0.0434
Inlet Section Slope: N.A.
Steep Section Slope: 0.571 m/m
Outlet Section Slope: 0.021 m/m
CULVERT PROFILE DATA
Type: Single Broken-Back
Inlet Station: 0.000 m
Inlet Elevation: 10.000 m
Lower Break Station: 10.000 m
Lower Break Elevation: 9.600 m
Outlet Station: 37.200 m
Outlet Elevation: 8.510 m

Experiment 27, test (a) results:

NEBRASKA DEPARTMENT OF ROADS
Broken-Back Culvert Analysis Program (BCAP)
PROJECT INFO
Project: Increasing Rougness
Station or Location: Experiment 27a
Date: 05/04/2006
CULVERT DATA
Discharge: .236 cms
Shape: Box
Material: Concrete
Size: 1-1.8 m x 1.8 m
Inlet Type: Headwall, Square Edge (90-45 deg.)
WATER SURFACE PROFILE
Inlet Depth: 0.12 m
Inlet Velocity: 1.09 m/s
Upper Break Depth: 0.12 m
Upper Break Velocity: 1.09 m/s
Lower Break Depth: 0.13 m
Lower Break Velocity: 1.04 m/s
Depth at End of Hydraulic Jump: N/A m
Velocity at End of Hydraulic Jump: N/A m/s
Depth at End of Hydraulic Jump: 0.06 m
Velocity at End of Hydraulic Jump: 2.27 m/s
OUTPUT DATA
Head Water Depth: 0.20 m
Inlet Control Elevation: 10.20 m
Break Control Elevation: 0 m
Critical Depth: 0.12 m
Tailwater Depth: 0.06 m
Hydraulic Jump? NO
Outlet Depth: 0.13 m
Outlet Velocity: 1.04 m/s
Outlet Froude No.: .9

Experiment 27, test (b) setup:

NEBRASKA DEPARTMENT OF ROADS
Broken-Back Culvert Analysis Program (BCAP)
PROJECT INFO
Project: Increasing Rougness
Station or Location: Experiment 27b
Date: 05 / 04 / 2006
DISCHARGE DATA
Minimum: 0.000 cms
Design Discharge: 0.236 cms
Maximum: 1.000 cms
Number of Barrels: 1
TAILWATER DATA
Type: Downstream
Channel Shape: Rectangle
Bottom Width: 1.80 m
Bottom Slope: 0.04 m/m
Roughness Coefficient: 0.012
CULVERT DATA
Type: Concrete Box
Span (per barrel): 1.80 m
Rise: 1.80 m
Inlet Type: Headwall, Square Edge (90-45 deg.)
Roughness Coefficient: 0.012
Outlet Section Roughness Coeff.: 0.0434
Inlet Section Slope: N.A.
Steep Section Slope: 0.79 m/m
Outlet Section Slope: 0.0401 m/m
CULVERT PROFILE DATA
Type: Single Broken-Back
Inlet Station: 0.000 m
Inlet Elevation: 17.500 m
Lower Break Station: 10.000 m
Lower Break Elevation: 9.600 m
Outlet Station: 37.200 m
Outlet Elevation: 8.510 m

Experiment 27, test (b) results:

NEBRASKA DEPARTMENT OF ROADS
Broken-Back Culvert Analysis Program (BCAP)
PROJECT INFO
Project: Increasing Rougness
Station or Location: Experiment 27b
Date: 05/04/2006
CULVERT DATA
Discharge: .236 cms
Shape: Box
Material: Concrete
Size: 1-1.8 m x 1.8 m
Inlet Type: Headwall, Square Edge (90-45 deg.)
WATER SURFACE PROFILE
Inlet Depth: 0.12 m
Inlet Velocity: 1.09 m/s
Upper Break Depth: 0.12 m
Upper Break Velocity: 1.09 m/s
Lower Break Depth: 0.05 m
Lower Break Velocity: 2.82 m/s
Depth at End of Hydraulic Jump: 1.20 m
Velocity at End of Hydraulic Jump: .80 m/s
Depth at End of Hydraulic Jump: 0.06 m
Velocity at End of Hydraulic Jump: 2.27 m/s
OUTPUT DATA
Head Water Depth: 0.12 m
Inlet Control Elevation: 17.62 m
Break Control Elevation: 0 m
Critical Depth: 0.12 m
Tailwater Depth: 0.06 m
Hydraulic Jump? YES
Jump Station: 10.76 m
Jump Length: 0.56 m
Outlet Depth: 0.12 m
Outlet Velocity: 1.09 m/s
Outlet Froude No.: 1.0

Experiment 40, test (a) setup:

NEBRASKA DEPARTMENT OF ROADS
Broken-Back Culvert Analysis Program (BCAP)
PROJECT INFO
Project: Increasing Rougness
Station or Location: Experiment 40a
Date: 05 / 04 / 2006
DISCHARGE DATA
Minimum: 0.000 cms
Design Discharge: 0.806 cms
Maximum: 1.000 cms
Number of Barrels: 1
TAILWATER DATA
Type: Downstream
Channel Shape: Rectangle
Bottom Width: 1.80 m
Bottom Slope: 0.06 m/m
Roughness Coefficient: 0.012
CULVERT DATA
Type: Concrete Box
Span (per barrel): 1.80 m
Rise: 1.80 m
Inlet Type: Headwall, Square Edge (90-45 deg.)
Roughness Coefficient: 0.012
Outlet Section Roughness Coeff.: 0.0347
Inlet Section Slope: N.A.
Steep Section Slope: 0.06 m/m
Outlet Section Slope: 0.0599 m/m
CULVERT PROFILE DATA
Type: Single Broken-Back
Inlet Station: 0.000 m
Inlet Elevation: 10.000 m
Lower Break Station: 10.000 m
Lower Break Elevation: 9.400 m
Outlet Station: 37.200 m
Outlet Elevation: 7.770 m

Experiment 40, test (a) results:

NEBRASKA DEPARTMENT OF ROADS
Broken-Back Culvert Analysis Program (BCAP)
PROJECT INFO
Project: Increasing Rougness
Station or Location: Experiment 40a
Date: 05/04/2006
CULVERT DATA
Discharge: .806 cms
Shape: Box
Material: Concrete
Size: 1-1.8 m x 1.8 m
Inlet Type: Headwall, Square Edge (90-45 deg.)
WATER SURFACE PROFILE
Inlet Depth: 0.27 m
Inlet Velocity: 1.64 m/s
Upper Break Depth: 0.27 m
Upper Break Velocity: 1.64 m/s
Lower Break Depth: 0.21 m
Lower Break Velocity: 2.18 m/s
Depth at End of Hydraulic Jump: N/A m
Velocity at End of Hydraulic Jump: N/A m/s
Depth at End of Hydraulic Jump: 0.11 m
Velocity at End of Hydraulic Jump: 4.20 m/s
OUTPUT DATA
Head Water Depth: 0.44 m
Inlet Control Elevation: 10.44 m
Break Control Elevation: 0 m
Critical Depth: 0.27 m
Tailwater Depth: 0.11 m
Hydraulic Jump? NO
Outlet Depth: 0.21 m
Outlet Velocity: 2.18 m/s
Outlet Froude No.: 1.5

Experiment 40, test (b) setup:

NEBRASKA DEPARTMENT OF ROADS
Broken-Back Culvert Analysis Program (BCAP)
PROJECT INFO
Project: Increasing Rougness
Station or Location: Experiment 40b
Date: 05 / 04 / 2006
DISCHARGE DATA
Minimum: 0.000 cms
Design Discharge: 0.806 cms
Maximum: 1.000 cms
Number of Barrels: 1
TAILWATER DATA
Type: Downstream
Channel Shape: Rectangle
Bottom Width: 1.80 m
Bottom Slope: 0.06 m/m
Roughness Coefficient: 0.012
CULVERT DATA
Type: Concrete Box
Span (per barrel): 1.80 m
Rise: 1.80 m
Inlet Type: Headwall, Square Edge (90-45 deg.)
Roughness Coefficient: 0.012
Outlet Section Roughness Coeff.: 0.0347
Inlet Section Slope: N.A.
Steep Section Slope: 0.41 m/m
Outlet Section Slope: 0.0599 m/m
CULVERT PROFILE DATA
Type: Single Broken-Back
Inlet Station: 0.000 m
Inlet Elevation: 13.500 m
Lower Break Station: 10.000 m
Lower Break Elevation: 9.400 m
Outlet Station: 37.200 m
Outlet Elevation: 7.770 m

Experiment 40, test (b) results:

NEBRASKA DEPARTMENT OF ROADS
Broken-Back Culvert Analysis Program (BCAP)
PROJECT INFO
Project: Increasing Rougness
Station or Location: Experiment 40b
Date: 05/04/2006
CULVERT DATA
Discharge: .806 cms
Shape: Box
Material: Concrete
Size: 1-1.8 m x 1.8 m
Inlet Type: Headwall, Square Edge (90-45 deg.)
WATER SURFACE PROFILE
Inlet Depth: 0.27 m
Inlet Velocity: 1.64 m/s
Upper Break Depth: 0.27 m
Upper Break Velocity: 1.64 m/s
Lower Break Depth: 0.11 m
Lower Break Velocity: 3.94 m/s
Depth at End of Hydraulic Jump: N/A m
Velocity at End of Hydraulic Jump: N/A m/s
Depth at End of Hydraulic Jump: 0.11 m
Velocity at End of Hydraulic Jump: 4.20 m/s
OUTPUT DATA
Head Water Depth: 0.33 m
Inlet Control Elevation: 13.83 m
Break Control Elevation: 0 m
Critical Depth: 0.27 m
Tailwater Depth: 0.11 m
Hydraulic Jump? NO
Outlet Depth: 0.21 m
Outlet Velocity: 2.18 m/s
Outlet Froude No.: 1.5

Experiment 40, test (c) setup:

NEBRASKA DEPARTMENT OF ROADS
Broken-Back Culvert Analysis Program (BCAP)
PROJECT INFO
Project: Increasing Rougness
Station or Location: Experiment 40c
Date: 05 / 04 / 2006
DISCHARGE DATA
Minimum: 0.000 cms
Design Discharge: 0.806 cms
Maximum: 1.000 cms
Number of Barrels: 1
TAILWATER DATA
Type: Downstream
Channel Shape: Rectangle
Bottom Width: 1.80 m
Bottom Slope: 0.06 m/m
Roughness Coefficient: 0.012
CULVERT DATA
Type: Concrete Box
Span (per barrel): 1.80 m
Rise: 1.80 m
Inlet Type: Headwall, Square Edge (90-45 deg.)
Roughness Coefficient: 0.012
Outlet Section Roughness Coeff.: 0.0347
Inlet Section Slope: N.A.
Steep Section Slope: 0.41 m/m
Outlet Section Slope: 0.0254 m/m
CULVERT PROFILE DATA
Type: Single Broken-Back
Inlet Station: 0.000 m
Inlet Elevation: 13.500 m
Lower Break Station: 10.000 m
Lower Break Elevation: 9.400 m
Outlet Station: 37.200 m
Outlet Elevation: 8.720 m

Experiment 40, test (c) results:

NEBRASKA DEPARTMENT OF ROADS
Broken-Back Culvert Analysis Program (BCAP)
PROJECT INFO
Project: Increasing Rougness
Station or Location: Experiment 40c
Date: 05/04/2006
CULVERT DATA
Discharge: .806 cms
Shape: Box
Material: Concrete
Size: 1-1.8 m x 1.8 m
Inlet Type: Headwall, Square Edge (90-45 deg.)
WATER SURFACE PROFILE
Inlet Depth: 0.27 m
Inlet Velocity: 1.64 m/s
Upper Break Depth: 0.27 m
Upper Break Velocity: 1.64 m/s
Lower Break Depth: 0.11 m
Lower Break Velocity: 3.94 m/s
Depth at End of Hydraulic Jump: 0.95 m
Velocity at End of Hydraulic Jump: 1.20 m/s
Depth at End of Hydraulic Jump: 0.11 m
Velocity at End of Hydraulic Jump: 4.20 m/s
OUTPUT DATA
Head Water Depth: 0.33 m
Inlet Control Elevation: 13.83 m
Break Control Elevation: 0 m
Critical Depth: 0.27 m
Tailwater Depth: 0.11 m
Hydraulic Jump? YES
Jump Station: 12.86 m
Jump Length: 1.33 m
Outlet Depth: 0.27 m
Outlet Velocity: 1.64 m/s
Outlet Froude No.: 1.0

APPENDIX I

RAW DATA FOR VELOCITY PROFILE EXPERIMENTS

Table I-1. Sampling positions for each experiment.

Experiment #	Sample #	Measurement #	Vertical Distance from Datum (ft)	Transverse Distance from Center (ft)
69	1	3	0.06	0.94
69	2	3	0.06	0.45
69	3	3	0.06	0.03
69	4	3	0.06	0.49
69	5	3	0.06	1.01
69	6	3	0.18	1.01
69	7	3	0.18	0.49
69	8	3	0.18	0.03
69	9	3	0.18	0.45
69	10	3	0.18	0.94
69	11	3	0.30	0.94
69	12	3	0.30	0.45
69	13	3	0.30	0.03
69	14	3	0.30	0.49
69	15	3	0.30	1.01
69	16	3c	0.17	1.01
69	17	3c	0.17	0.49
69	18	3c	0.17	0.03
69	19	3c	0.17	0.45
69	20	3c	0.17	0.94
69	21	3c	0.28	0.94
69	22	3c	0.28	0.45
69	23	3c	0.28	0.03
69	24	3c	0.28	0.49
69	25	3c	0.28	1.01
70	1	3	0.09	0.97
70	2	3	0.09	0.48
70	3	3	0.09	0
70	4	3	0.09	0.48
70	5	3	0.09	0.97
70	6	3	0.24	0.97
70	7	3	0.24	0.48
70	8	3	0.24	0
70	9	3	0.24	0.48
70	10	3	0.24	0.97

Table I-1 (continued).

Experiment #	Sample #	Measurement #	Vertical Distance from Datum (ft)	Transverse Distance from Center (ft)
70	11	3	0.39	0.97
70	12	3	0.39	0.48
70	13	3	0.39	0
70	14	3	0.39	0.48
70	15	3	0.39	0.97
70	16	3c	0.21	0.97
70	17	3c	0.21	0.48
70	18	3c	0.21	0
70	19	3c	0.21	0.48
70	20	3c	0.21	0.97
70	21	3c	0.36	0.97
70	22	3c	0.36	0.48
70	23	3c	0.36	0
70	24	3c	0.36	0.48
70	25	3c	0.36	0.97
71	1	3	0.05	1.14
71	2	3	0.05	0.61
71	3	3	0.05	0.08
71	4	3	0.05	0.45
71	5	3	0.05	0.99
71	6	3	0.16	0.99
71	7	3	0.16	0.45
71	8	3	0.16	0.08
71	9	3	0.16	0.61
71	10	3	0.16	1.14
71	11	3	0.27	1.14
71	12	3	0.27	0.61
71	13	3	0.27	0.08
71	14	3	0.27	0.45
71	15	3	0.27	0.99
71	16	3c	0.16	1.03
71	17	3c	0.16	0.51
71	18	3c	0.16	0.01
71	19	3c	0.16	0.53
71	20	3c	0.16	1.04
71	21	3c	0.28	1.04
71	22	3c	0.28	0.53
71	23	3c	0.28	0.01
71	24	3c	0.28	0.51
71	25	3c	0.28	1.03
72	1	3	0.12	1.11

Table I-1 (continued).

Experiment #	Sample #	Measurement #	Vertical Distance from Datum (ft)	Transverse Distance from Center (ft)
72	2	3	0.12	0.58
72	3	3	0.12	0.05
72	4	3	0.12	0.48
72	5	3	0.12	1.02
72	6	3	0.21	1.02
72	7	3	0.21	0.48
72	8	3	0.21	0.05
72	9	3	0.21	0.58
72	10	3	0.21	1.11
72	11	3	0.30	1.11
72	12	3	0.30	0.58
72	13	3	0.30	0.05
72	14	3	0.30	0.48
72	15	3	0.30	1.02
72	16	3c	0.14	1.14
72	17	3c	0.14	0.60
72	18	3c	0.14	0.06
72	19	3c	0.14	0.48
72	20	3c	0.14	1.03
72	21	3c	0.22	1.03
72	22	3c	0.22	0.48
72	23	3c	0.22	0.06
72	24	3c	0.22	0.60
72	25	3c	0.22	1.14
73	1	3	0.09	1.14
73	2	3	0.09	0.56
73	3	3	0.09	0.02
73	4	3	0.09	0.60
73	5	3	0.09	1.18
73	6	3	0.24	1.18
73	7	3	0.24	0.60
73	8	3	0.24	0.02
73	9	3	0.24	0.56
73	10	3	0.24	1.14
73	11	3	0.39	1.14
73	12	3	0.39	0.56
73	13	3	0.39	0.02
73	14	3	0.39	0.06
73	15	3	0.39	1.18
73	16	3c	0.22	1.14
73	17	3c	0.22	0.56

Table I-1 (continued).

Experiment #	Sample #	Measurement #	Vertical Distance from Datum (ft)	Transverse Distance from Center (ft)
73	18	3c	0.22	0.02
73	19	3c	0.22	0.60
73	20	3c	0.22	1.18
73	21	3c	0.38	1.18
73	22	3c	0.38	0.60
73	23	3c	0.38	0.02
73	24	3c	0.38	0.56
73	25	3c	0.38	1.14
74	1	3	0.07	1.15
74	2	3	0.07	0.57
74	3	3	0.07	0.01
74	4	3	0.07	0.59
74	5	3	0.07	1.16
74	6	3	0.20	1.16
74	7	3	0.20	0.59
74	8	3	0.20	0.01
74	9	3	0.20	0.57
74	10	3	0.20	1.15
74	11	3	0.33	1.15
74	12	3	0.33	0.57
74	13	3	0.33	0.01
74	14	3	0.33	0.59
74	15	3	0.33	1.16
74	16	3	0.46	1.16
74	17	3	0.46	0.59
74	18	3	0.46	0.01
74	19	3	0.46	0.57
74	20	3	0.46	1.15
74	21	3	0.59	1.15
74	22	3	0.59	0.57
74	23	3	0.59	0.01
74	24	3	0.59	0.59
74	25	3	0.59	1.16
74	26	3	0.72	1.16
74	27	3	0.72	0.59
74	28	3	0.72	0.01
74	29	3	0.72	0.57
74	30	3	0.72	1.15
74	31	3c	0.21	1.15
74	32	3c	0.21	0.57
74	33	3c	0.21	0.01

Table I-1 (continued).

Experiment #	Sample #	Measurement #	Vertical Distance from Datum (ft)	Transverse Distance from Center (ft)
74	34	3c	0.21	0.59
74	35	3c	0.21	1.16
74	36	3c	0.36	1.16
74	37	3c	0.36	0.59
74	38	3c	0.36	0.01
74	39	3c	0.36	0.57
74	40	3c	0.36	1.15
74	41	3c	0.51	1.15
74	42	3c	0.51	0.57
74	43	3c	0.51	0.01
74	44	3c	0.51	0.59
74	45	3c	0.51	1.16
74	46	3c	0.66	1.16
74	47	3c	0.66	0.59
74	48	3c	0.66	0.01
74	49	3c	0.66	0.57
74	50	3c	0.66	1.15
75	1	3	-0.02	0
75	2	3	0.02	0
75	3	3	0.06	0
75	4	3	0.10	0
75	5	3	0.14	0
75	6	3	0.18	0
75	7	3	0.22	0
75	8	3	0.26	0
75	9	3	0.30	0
75	10	3	0.34	0
75	11	3	0.38	0
75	12	3	0.42	0
75	13	3	0.46	0
75	14	3c	0.09	0
75	15	3c	0.12	0
75	16	3c	0.15	0
75	17	3c	0.18	0
75	18	3c	0.21	0
75	19	3c	0.24	0
75	20	3c	0.27	0
75	21	3c	0.30	0
75	22	3c	0.33	0
75	23	3c	0.36	0
75	24	3c	0.39	0

Table I-1 (continued).

Experiment #	Sample #	Measurement #	Vertical Distance from Datum (ft)	Transverse Distance from Center (ft)
75	25	3c	0.42	0
75	26	3c	0.45	0
76	1	3	-0.03	0
76	2	3	0.00	0
76	3	3	0.03	0
76	4	3	0.06	0
76	5	3	0.09	0
76	6	3	0.12	0
76	7	3	0.15	0
76	8	3	0.18	0
76	9	3	0.21	0
76	10	3	0.24	0
76	11	3	0.27	0
76	12	3	0.30	0
76	13	3c	0.09	0
76	14	3c	0.12	0
76	15	3c	0.15	0
76	16	3c	0.18	0
76	17	3c	0.21	0
76	18	3c	0.24	0
76	19	3c	0.27	0
76	20	3c	0.30	0
77	1	3	-0.03	0
77	2	3	0.00	0
77	3	3	0.03	0
77	4	3	0.06	0
77	5	3	0.09	0
77	6	3	0.12	0
77	7	3	0.15	0
77	8	3	0.18	0
77	9	3	0.21	0
77	10	3	0.24	0
77	11	3	0.27	0
77	12	3c	0.09	0
77	13	3c	0.12	0
77	14	3c	0.15	0
77	15	3c	0.18	0
77	16	3c	0.21	0
77	17	3c	0.24	0
77	18	3c	0.27	0
78	1	3	-0.02	0

Table I-1 (continued).

Experiment #	Sample #	Measurement #	Vertical Distance from Datum (ft)	Transverse Distance from Center (ft)
78	2	3	0.02	0
78	3	3	0.06	0
78	4	3	0.10	0
78	5	3	0.14	0
78	6	3	0.18	0
78	7	3	0.22	0
78	8	3	0.26	0
78	9	3	0.30	0
78	10	3	0.34	0
78	11	3	0.38	0
78	12	3c	0.09	0
78	13	3c	0.12	0
78	14	3c	0.15	0
78	15	3c	0.18	0
78	16	3c	0.21	0
78	17	3c	0.24	0
78	18	3c	0.27	0
78	19	3c	0.30	0
78	20	3c	0.33	0

Table I-2. SNR and average streamwise velocity for each sample.

Experiment #	Sample #	SNR (dB)	Streamwise velocity (cm/s)
69	1	21.8	-4.57
69	2	22.1	0.88
69	3	19.1	-3.02
69	4	16.0	-15.9
69	5	16.6	-10.7
69	6	20.0	6.65
69	7	20.3	9.59
69	8	20.4	17.1
69	9	20.4	24.9
69	10	21.0	25.1
69	11	5.89	47.4
69	12	0.56	-
69	13	1.06	-
69	14	7.70	45.5
69	15	21.0	77.0
69	16	16.3	-2.31
69	17	15.3	10.8
69	18	12.6	-31.6
69	19	14.8	20.4
69	20	17.9	23.4
69	21	7.42	42.7
69	22	1.61	-
69	23	2.16	-
69	24	13.2	18.9
69	25	21.2	40.4
70	1	26.0	-13.8
70	2	28.2	-11.8
70	3	42.3	-7.03
70	4	56.3	0.95
70	5	47.9	0.35
70	6	24.3	65.3
70	7	23.7	73.2
70	8	23.5	75.3
70	9	23.6	77.5
70	10	24.2	84.2

Table I-2 (continued).

Experiment #	Sample #	SNR (dB)	Streamwise velocity (cm/s)
70	11	2.54	-
70	12	1.10	-
70	13	1.46	-
70	14	1.48	-
70	15	3.61	-
70	16	40.3	14.7
70	17	50.5	6.96
70	18	48.2	17.5
70	19	31.2	29.2
70	20	26.1	58.3
70	21	9.85	74.4
70	22	1.93	-
70	23	1.70	-
70	24	2.71	-
70	25	9.81	69.2
71	1	43.2	-0.11
71	2	37.6	-6.38
71	3	20.5	-3.85
71	4	18.4	-42.4
71	5	21.3	-12.8
71	6	25.1	-18.4
71	7	10.6	0.50
71	8	17.1	1.87
71	9	10.7	7.24
71	10	17.9	21.0
71	11	6.18	36.0
71	12	0.57	-
71	13	0.79	-
71	14	0.65	-
71	15	1.64	-
71	16	22.7	25.7
71	17	13.5	7.75
71	18	17.8	7.79
71	19	14.8	21.0
71	20	13.0	25.2
71	21	0.88	-
71	22	0.64	-
71	23	0.96	-
71	24	0.74	-
71	25	2.29	-
72	1	15.9	-12.2

Table I-2 (continued).

Experiment #	Sample #	SNR (dB)	Streamwise velocity (cm/s)
72	2	15.5	-23.7
72	3	19.9	-15.4
72	4	13.9	16.2
72	5	27.6	-15.9
72	6	23.9	-17.6
72	7	20.6	-7.41
72	8	20.8	-10.7
72	9	19.9	-12.8
72	10	19.2	-10.4
72	11	10.8	56.6
72	12	0.41	-
72	13	0.53	-
72	14	0.88	-
72	15	2.01	-
72	16	12.8	-92.3
72	17	12.3	8.92
72	18	21.3	9.49
72	19	35.5	1.56
72	20	25.4	-0.53
72	21	1.23	-
72	22	1.12	-
72	23	1.43	-
72	24	1.54	-
72	25	12.8	38.6
73	1	21.1	-18.8
73	2	39.8	9.09
73	3	53.5	0.62
73	4	32.9	-1.89
73	5	17.2	-2.99
73	6	17.4	41.2
73	7	16.6	43.6
73	8	15.4	39.9
73	9	13.6	30.6
73	10	15.2	25.8
73	11	16.8	47.1
73	12	14.7	44.2
73	13	16.6	51.0
73	14	18.3	60.3
73	15	18.6	54.5
73	16	40.8	8.16
73	17	46.8	5.32

Table I-2 (continued).

Experiment #	Sample #	SNR (dB)	Streamwise velocity (cm/s)
73	18	30.4	13.6
73	19	18.2	24.3
73	20	16.6	39.4
73	21	18.4	51.9
73	22	17.5	55.9
73	23	16.5	49.4
73	24	15.1	46.2
73	25	15.7	47.8
74	1	16.8	-13.1
74	2	11.1	2.54
74	3	15.0	-0.13
74	4	25.0	-2.34
74	5	40.0	-11.7
74	6	19.7	31.0
74	7	18.3	17.3
74	8	17.6	6.78
74	9	19.4	2.60
74	10	21.4	9.41
74	11	21.5	53.5
74	12	21.2	59.8
74	13	20.7	55.3
74	14	18.8	42.3
74	15	20.0	50.9
74	16	20.2	54.6
74	17	18.8	46.5
74	18	20.8	58.6
74	19	21.6	59.6
74	20	20.4	53.9
74	21	21.3	68.5
74	22	20.9	68.5
74	23	20.6	65.5
74	24	20.6	60.3
74	25	21.6	61.8
74	26	22.5	58.6
74	27	20.0	61.9
74	28	4.73	-
74	29	15.4	65.5
74	30	22.9	68.3
74	31	14.3	12.7
74	32	15.4	17.4
74	33	12.1	16.1

Table I-2 (continued).

Experiment #	Sample #	SNR (dB)	Streamwise velocity (cm/s)
74	34	19.6	13.2
74	35	20.5	31.6
74	36	20.9	54.0
74	37	20.1	53.4
74	38	21.0	65.3
74	39	21.1	70.3
74	40	21.2	62.0
74	41	21.9	68.9
74	42	22.2	78.7
74	43	21.3	69.2
74	44	20.3	54.9
74	45	20.9	54.1
74	46	21.2	54.7
74	47	21.0	58.5
74	48	21.7	70.1
74	49	22.5	79.3
74	50	22.5	71.2
75	1	22.4	-5.34
75	2	33.2	-1.71
75	3	16.2	-4.04
75	4	44.4	-3.00
75	5	16.7	-14.9
75	6	17.0	9.42
75	7	17.1	50.6
75	8	17.4	62.0
75	9	17.5	69.9
75	10	17.9	75.1
75	11	11.9	77.2
75	12	2.15	-
75	13	4.69	-
75	14	21.8	-1.28
75	15	28.5	1.10
75	16	11.6	-5.11
75	17	18.1	4.75
75	18	39.0	13.5
75	19	16.9	56.4
75	20	17.1	44.5
75	21	17.2	69.1
75	22	17.3	73.3
75	23	17.5	76.7
75	24	6.67	68.5

Table I-2 (continued).

Experiment #	Sample #	SNR (dB)	Streamwise velocity (cm/s)
75	25	1.77	-
75	26	2.54	-
76	1	21.4	1.93
76	2	33.1	-2.31
76	3	9.31	-42.6
76	4	23.6	-28.0
76	5	39.9	-4.88
76	6	12.8	-8.38
76	7	13.0	3.03
76	8	13.0	15.1
76	9	13.2	35.4
76	10	13.6	48.5
76	11	13.8	53.0
76	12	3.74	-
76	13	15.5	8.14
76	14	26.3	-0.36
76	15	7.93	-116
76	16	13.9	9.43
76	17	42.6	8.34
76	18	13.8	41.5
76	19	14.1	36.3
76	20	1.46	-
77	1	21.7	1.07
77	2	30.8	4.39
77	3	13.5	4.15
77	4	26.6	-1.56
77	5	43.6	-4.80
77	6	19.6	-10.2
77	7	18.5	2.26
77	8	6.81	5.73
77	9	0.74	-
77	10	0.42	-
77	11	3.31	-
77	12	16.5	7.45
77	13	21.3	-0.64
77	14	13.5	-14.8
77	15	7.63	8.45
77	16	1.61	-
77	17	1.11	-
77	18	5.72	28.2
78	1	27.0	-0.35

Table I-2 (continued).

Experiment #	Sample #	SNR (dB)	Streamwise velocity (cm/s)
78	2	23.2	1.62
78	3	19.0	-17.9
78	4	50.5	-0.69
78	5	20.8	-15.5
78	6	18.4	6.78
78	7	11.8	32.2
78	8	3.86	-
78	9	0.87	-
78	10	0.65	-
78	11	4.31	-
78	12	14.6	-8.32
78	13	26.8	1.61
78	14	15.4	7.65
78	15	20.3	25.9
78	16	17.0	6.81
78	17	2.08	-
78	18	0.78	-
78	19	0.51	-
78	20	1.02	-